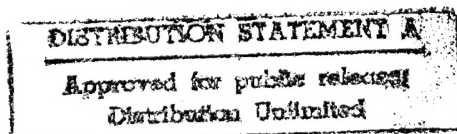Physiologically-Based Pharmacokinetic Modeling

of Skin Absorption Using Dermal Subcompartments

THESIS
Richard Lynn Bookout Jr.
First Lieutenant, USAF

AFIT/GCS/ENC/95J-01

DTIC QUALITY INSPECTED 5

DEPARTMENT OF THE AIR FORCE

AIR UNIVERSITY

AIR FORCE INSTITUTE OF TECHNOLOGY

Wright-Patterson Air Force Base, Ohio

19950811 045

Physiologically-Based Pharmacokinetic Modeling

of Skin Absorption Using Dermal Subcompartments

THESIS
Richard Lynn Bookout Jr.
First Lieutenant, USAF

AFIT/GCS/ENC/95J-01

The views expressed in this thesis are those of the author and do not reflect the official policy or position of the Department of Defense or the U. S. Government.

Accession For

NTIS GRA&I	☑
DTIC TAB	☐
Unannounced	☐
Justification

By

Distribution/

| Availability Codes |
| Dist | Avail and/or Special |
| A-1 | |

AFIT/GCS/ENC/95J-01

Physiologically-Based Pharmacokinetic Modeling

of Skin Absorption Using Dermal Subcompartments

THESIS

Presented to the Faculty of the School of Engineering

of the Air Force Institute of Technology

Air University

In Partial Fulfillment of the

Requirements for the Degree of

Master of Science in Computer Systems

Richard Lynn Bookout Jr., B.S.

First Lieutenant, USAF

June, 1995

Table of Contents

List of Figures

List of Tables

AFIT/GCS/ENC/95J-01

Abstract

Dermal penetration of chemicals and drugs is important to both toxicologists and pharmacologists. Drug developers try to enhance and environmental professionals try to limit penetration of chemicals through the skin. Both can use predictive biologically-based mathematical models to assist in understanding the processes involved. When these models are based on physiological and biochemical parameters which can be measured in the laboratory, they can be extremely useful. Appropriately validated models based on first principles can be predictive of human exposures when the processes involved are adequately understood. In this thesis we develop four new physiologically-based pharmacokinetic (PBPK) models to predict blood concentrations of dibromomethane (DBM) in rats after neat liquid and vapor exposure. These four new models expand previously developed homogeneous models by adding skin subcompartments. These new models improve the prediction of the blood concentrations especially early in the exposure. Sensitivity analysis shows that one of the permeability constants followed by the blood air partition coefficient have the most impact on blood concentration predictions. With proper validation the new models could be used to improve species, dose, and duration extrapolations of chemical or drug penetration. They could also be used to investigate and predict concentrations of drugs or chemicals in different parts of the skin.

Physiologically-Based Pharmacokinetic Modeling
of Skin Absorption Using Dermal Subcompartments

I. Introduction

1.1 Overview

The effect a chemical will have on the human body is usually unknown until actual experiments are conducted on humans. This can be a dangerous proposition due to the toxic hazards of some chemicals, thus a method of predicting these effects would greatly decrease this danger. One method to make these predictions is to conduct experiments using laboratory animals and try to extrapolate the results across species to predict the effect on humans. Many researchers have developed mathematical models to simulate the physical and chemical processes in the body. A physiologically-based pharmacokinetic (PBPK) model is one such model which uses mathematical equations to represent the flow of a chemical through the body. Some applications of PBPK models include modeling inhalation exposure, vapor dermal exposure, and liquid dermal exposure. The equations of a PBPK model contain physiological and biochemical parameters that can be measured in the laboratory or estimated. Using parameters that can be measured in humans, as well as, laboratory animals allows for the possibility of the results to be extrapolated across species. It can be difficult to model dermal absorption because of the complex nature of the skin and its penetrability. Models which include more detailed equations representing the skin and its subcompartments can lead to improved model predictions and improve the possibility of extrapolating the results. Sensitivity analysis can identify the parameters of a model that have the most significant impact on the model output, which reveals the most important parameters to measure in the laboratory or estimate if necessary.

1.2 Problem

It is important for the Air Force to be able to predict the effect of chemicals on humans, which includes determining the concentration of the chemical in various parts of the body after exposure. Models have been developed that predict blood concentrations in rats relatively well, however more detailed models that use dermal subcompartments and are based on biological parameters can give more accurate predictions and make extrapolation across species to humans easier.

1.3 Scope

This research expands current PBPK models to include dermal subcompartments in series and parallel. The models developed simulate percutaneous absorption of dibromomethane (DBM) vapor and neat DBM liquid. The model determines the concentration of the chemicals in various parts of the body and does not account for the physical change the chemical may cause to the skin. Some of the new model parameters that were unable to be measured had to be optimized. When techniques to measure these parameter values in the laboratory become available, the estimates can be replaced with the actual values. The accuracy of the models is based on comparisons made between the models' output and experimental data collected in the laboratory from experiments involving rats. Metabolism in the liver is the only form of metabolism that is represented in this model. The model results have not been extrapolated across species to predict effects on humans, however the model parameters were chosen so that future extrapolation should be possible. Sensitivity analysis was performed to identify the most important parameters to measure or estimate.

1.4 Approach

This research created new models that predict blood concentration profiles of chemicals after percutaneous absorption. In this thesis, we

1. Reconstructed a previously published vapor model and verified the results using previously collected laboratory animal data for DBM.

2. Reconstructed a previously developed neat liquid model and verified the results using previously collected animal data for DBM.

3. Reconstructed a previously developed layered subcompartment vapor model and added a few additional constraints.

4. Extended the vapor model to include a parallel follicle compartment.

5. Combined the layered subcompartment approach and the parallel subcompartment approach into one new model for the vapor exposure.

6. Extended the neat liquid model to include separate subcompartments representing distinct layers of the skin.

7. Extended the neat liquid model to include a parallel follicle compartment.

8. Combined the layered subcompartment approach and the parallel subcompartment approach into one new model for the neat liquid exposure.

9. Compared all of the models to previously collected experimental data with graphical plots and a calculated sum of squared deviations.

10. Performed sensitivity analysis on the models and identified the most important model parameters to be measured or estimated.

1.5 Design Considerations

The new models developed in this research should be able to predict blood concentration profiles of chemicals other than the ones discussed in this thesis by using the corresponding biochemical parameters. We chose DBM to use in the validation of the models because it is one of the chemicals that the Toxicology Division of the Armstrong Laboratory is currently interested in modeling [24]. The new parameters derived in the new models are biological-based so the parameters should be measurable in humans so the results can be extrapolated across species.

1.6 Summary of Thesis

The thesis is organized as follows:

Chapter II reviews the fundamentals of skin absorption and physiologically-based pharmacokinetic (PBPK) modeling. It also includes a discussion of the previous and current research being done in this area.

Chapter III presents the model design and implementation.

Chapter IV presents the results of the new models compared to animal data previously collected in the laboratory. It also includes sensitivity analysis which identifies the parameters that have the largest impact on the model output.

Chapter V presents a summary of the work completed and gives the conclusions reached. It also includes recommendations for future research.

II. Background

2.1 Overview

Both pharmacologists and toxicologists are concerned with the absorption of chemicals through the skin. The ability to predict the concentration of a chemical in various parts of the body following percutaneous absorption, which is the absorption of chemicals through the skin, can be obtained with a good understanding the absorption process. To fully understand percutaneous absorption one must first understand the complex structure and function of the skin. There are many things that affect the permeability of the skin including regional and structural variations and chemical properties. Pharmacokinetic models can be developed to simulate the pharmacokinetics (absorption, distribution, metabolism, and elimination) of a chemical in the body.

Not all models use the same approach to represent diffusion through the skin. Models that include biologically-based parameters that can be measured in different species have the best chance for extrapolation. Models based on mathematics alone can be very accurate for the specific conditions for which they are created, but extrapolation to other conditions and species can be extremely difficult. Physiologically-based pharmacokinetic (PBPK) models are based on physiological and biological parameters that can be measured in different species. Sensitivity analysis of PBPK models can be used to identify the most important biologically-based parameters to measure.

Before explaining our model design and implementation, we will review the structure of mammalian skin, some previous work, PBPK modeling, a previously developed dermal vapor absorption model, and a previously developed dermal layered subcompartment model.

2.2 Skin Structure

The skin is a very important part of our body. The skin is the largest organ in the body by weight and is the primary means of identifying individuals. The entire body is enveloped by the skin allowing it to protect the body from the outside environment which is its most important function. Bodily fluids would escape and external fluids would enter the body much easier if the skin was not present. An animal's skin enables it in certain ways to communicate, respond, and adapt to its environment. The skin can protect, camouflage, warn, or attract attention, and in some animals its glands can secrete substances that can repel or attract other animals [26].

The skin has many detailed structural and functional differences among various species but the overall effect of the skin on the body is the same in all species [26]. Certain characteristics of the skin vary over different regions of the body implying the skin is not a uniform organ. For example, the thickness and permeability of the skin differs greatly from some areas of the body to others [46]. The skin is as thick as 400-600 μ in plantar and palmer callus versus 10-20 μ thick on the back, arms, legs, and abdomen [30]. The number of skin appendages and other structures also vary across the body.

2.2.1 Skin Layers. Most people normally think of the skin as a single-layered membrane that covers and protects the body. A more detailed description identifies two distinct but linked layers which contain sublayers within them. The outer layer is the epidermis and the inner layer is known as the dermis or cornium [33]. Figure 2.1 shows a cross section of the skin revealing its complex structure.

The epidermis contains two parts, the stratum corneum and the viable epidermis. The stratum corneum is the outermost part of the epidermis and often referred to as the horny layer of the skin. The stratum corneum is made up of layers of non-living cells which are constantly being replaced. These non-living cells originate
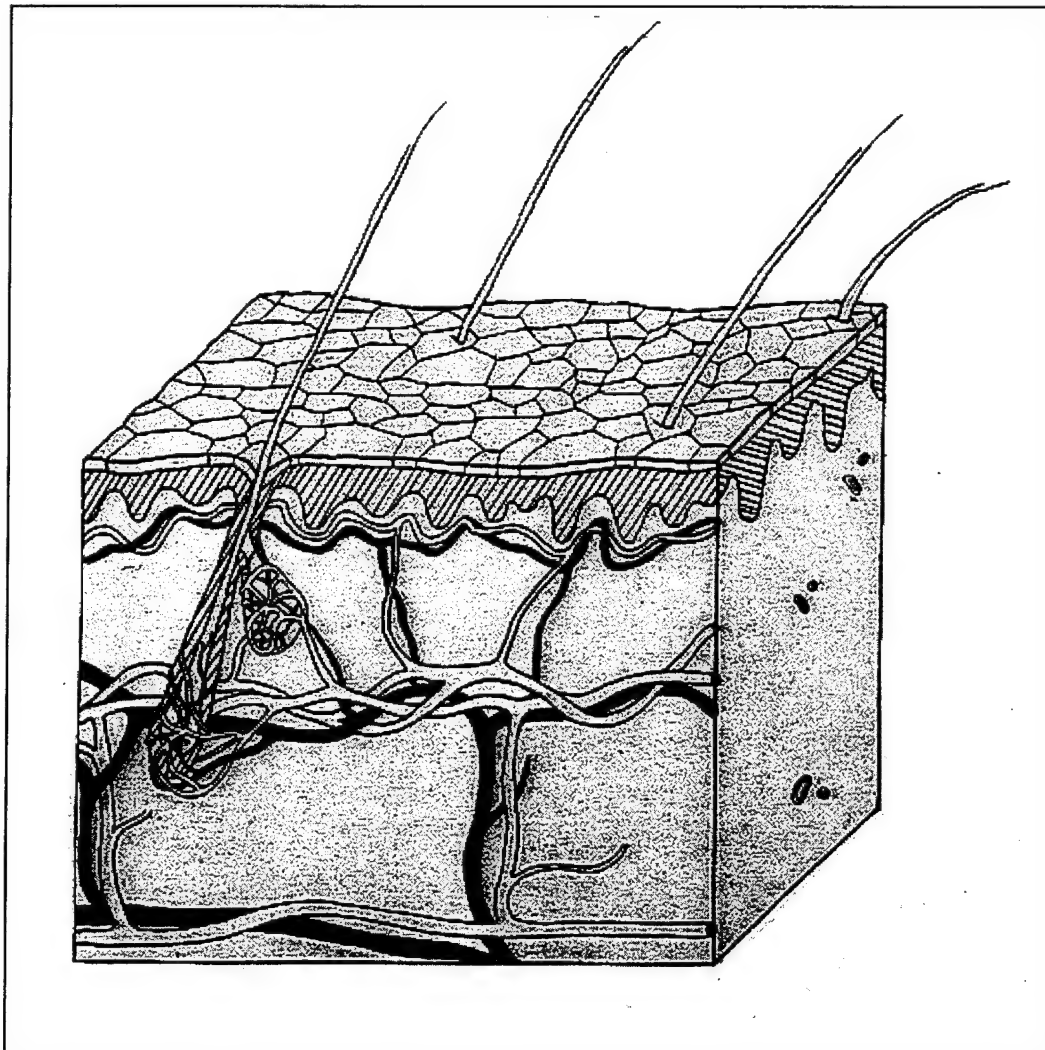
Figure 2.1   Cross section view of the skin

in the germinative basal layer of the epidermis and gradually move upwards replenishing the stratum corneum about every two to four weeks [25, 33]. The stratum corneum is the main barrier to penetration through the skin [36]. The viable epidermis not only supplies the dead cells to the stratum corneum but it also surrounds hair follicles, even into lower skin layers. The epidermal layer makes up about 25 percent of the total skin thickness [32].

The dermis or cornium is the inner layer of the skin which accounts for the bulk of the skin thickness and about 15 to 20 percent of the total body weight. The dermis is a matrix of loose connective tissue which is traversed by blood vessels, nerves, and lymphatics. The dermis is also penetrated from above by hair follicles and sweat glands. This tough, resilient and viscoelastic tissue has many functions which include providing nourishment to the epidermis [26].

2.2.2 Skin Appendages. A relatively small fractional area, approximately 10^{-3} in humans, of the skin is covered with skin appendages. Skin appendages include hair follicles, sweat ducts, and sebaceous glands [36]. These appendages help to regulate body temperature by sweating through the sweat glands. The hair that grows from hair follicles helps keep the body warm by providing a layer of insulation. The number of skin appendages varies from one species to another and from one region of the body to another. The skin appendages extend from the surface of the skin into and through the dermis where a dense capillary mesh surrounds them [35].

2.2.3 Skin Permeability. Skin permeability is important to understand when concerned with skin absorption because it determines how much the body accumulates or eliminates substances through the skin. Skin permeability varies across the body with the regional variations in the physiological properties of the skin [38]. The skin permeability is also different in each layer of the skin, the stratum corneum being the least permeable layer. In places where the skin is diseased, damaged, or removed, absorption of water-soluble chemicals can be 1,000 times

greater than normal. Even through normal intact skin, there can be a huge difference in the absorption of chemicals with different properties [36]. These variances in skin permeability make modeling skin absorption very challenging.

2.3 Classical Pharmacokinetic Modeling

Laboratory animals are often used in experiments to determine the effect of percutaneously absorbed chemicals. Chemical concentration in blood taken from the animals at set times after exposure gives some indication of the processes taking place. These *in vivo* techniques give a more complete analysis than *in vitro* techniques since metabolism, nervous, and humoral responses are not present in *in vitro* experiments [21]. It is important to be able to develop models that make predictions consistent with the data from *in vivo* experiments so fewer laboratory animals will have to be sacrificed. These models can be used to predict the effect of chemicals on humans.

There are two basic types of models that have been used for modeling percutaneous absorption, one is the compartment model [12, 45] which is based on first-order rate constants and the other is the diffusion model which is based on the diffusion laws. The diffusion model has been used most often when modeling absorption of solutes through the skin and it is the most correct mechanistically [40].

The mathematics used to describe skin permeability in the diffusion model are based on Fick's second law which is presented in Equation (2.1).

$$\frac{\partial C}{\partial t} = D\frac{\partial^2 C}{\partial x^2} \tag{2.1}$$

Where

C = Concentration

t = Time

D = Average membrane diffusion coefficient (distance^2 time^{-1})

x = Distance

The following integrated form of Fick's law represents the steady-state flux of solute [36].

$$J_s = \frac{D \cdot (C_1 - C_2)}{\delta} \qquad (2.2)$$

Where

J_s = Steady-state flux of solute (moles distance^{-2} time^{-1})

δ = membrane thickness (cm)

It is also necessary to include a term to describe the relationship between external and surface concentrations which can be done using the solvent-membrane distribution coefficient (K_m). Including this coefficient, Equation (2.2) becomes the following.

$$J_s = \frac{K_m \cdot D \cdot \Delta C_s}{\delta} \qquad (2.3)$$

Where

ΔC_s = Concentration difference of solute across membrane (moles cm^{-3})

K_m = (Solute sorbed per cc of tissue)/(Solute in solution per cc of solvent)

The permeability coefficient (k_p) is described using a portion of this flux equation and is normally used in a model. The permeability coefficient describes the rate of absorption of the chemical (distance/time).

$$k_p = \frac{K_m \cdot D}{\delta} \qquad (2.4)$$

Where

2-6

k_p = Permeability constant for solute (distance time^{-1})

The effective permeability of each skin layer relative to the permeability of the whole skin can be obtained. The following equation shows the relationship between the permeability constants for the individual skin layers and the permeability constant for the whole skin [5, 34].

$$\frac{1}{k_{p_{sk}}} = \sum_i \frac{1}{k_{p_i}}$$ (2.5)

Where

$k_{p_{sk}}$ = Permeability constant of the whole skin

k_{p_i} = Permeability constant for the ith layer of the skin

Several mathematical models have been developed that represent the absorption of chemicals through the skin using a layered subcompartment approach. Some of the layered models use two [11, 27, 41, 45] or three [40] subcompartments.

The skin appendages act as diffusional shunts for penetration through the skin. Solutions penetrating the skin through the skin appendages by-pass the upper layers of the skin, thus exhibiting different permeability characteristics from the rest of the skin. The effect of parallel pathways on permeability relative to the whole skin can theoretically be obtained. The following equation shows the relationship between permeability constants for the parallel pathways and the permeability constant for the whole skin [7].

$$k_{p_{sk}} \cdot A_{sk} = \sum_i (k_{p_i} \cdot A_i)$$ (2.6)

Where

A_{sk} = Area of the whole skin

k_{p_i} = Permeability constant for the ith parallel pathway of the skin

2-7

A_i = Area of the ith parallel pathway of the skin

Many researchers have also investigated the effect of skin appendages as a shunt pathway in percutaneous absorption [14, 17, 35, 15, 43, 44]. Although researchers agree that appendages act as a diffusional shunt through the skin, the impact of appendages on percutaneous absorption varies, and is related to the intrinsic physical properties of the chemical tested and the time of application [14]. During the initial stage of absorption, the appendages may have a significant contribution, however once the chemical penetrates the stratum corneum and the viable epidermis, the contribution of the appendages to the overall absorption process is insignificant [17]. Experiments have revealed that differences in skin structure, for example skin appendages, could have an effect on percutaneous absorption when a slowly absorbed test penetrant is used [37]. Some mathematical models have been developed which contain a parallel skin subcompartment to represent a shunt pathway for chemicals penetrating the skin through skin appendages [2, 4, 18, 45].

Different approaches have been taken to represent the diffusion equations within the context of a model. Some models use partial differential equations, solving them with Laplace transformations [1, 10, 27, 47]. This approach allows the skin concentration to vary with skin depth and with time. These partial differential equations make it difficult to use biologically-based parameters and they have boundary conditions that can be difficult to incorporate into a model.

Most of the previously developed models mentioned above are primarily descriptive because they are based on classical pharmacokinetic techniques and other techniques that are not based on biological parameters which can be measured or estimated for the purpose of extrapolation from one species to another. Most of the time, the equations in these models are fit to a curve of the experimental data and are only useful for certain chemicals, species, and exposure concentrations. Since these models are based on mathematical analysis alone, they do not give a good biological description of the skin or the processes that take place within it. Another

type of model has been developed that is based more on physiological properties but contains the mathematics to describe the diffusion process accurately.

2.4 Physiologically-Based Pharmacokinetic Modeling

Using the experimental data to predict the effect of the chemical on other species is challenging. One tool used to make these predictions is a mathematical model which includes physiological and pharmacokinetic principles. A physiologically-based pharmacokinetic (PBPK) model is one such model which uses mathematical equations to describe the dynamics of chemicals moving through the body. A PBPK model can represent some of the nonlinear processes in the body by using physiological parameters such as blood flow rates, breathing rates, blood volumes, tissue volumes, permeability of membranes, and partitioning of chemicals into tissues [21, 42].

Some of the parameters in a PBPK model can be measured in a laboratory, however some of the parameters must be estimated to complete the model. One technique for estimating the unknown parameters is to optimize the unknown parameters in the model to get the best fit to the corresponding experimental data. These estimated values can be used until actual measurements can be made in the laboratory.

2.4.1 Mass-Balance Equations. PBPK models represent the body by identifying tissue compartments made up of single organs or groups of physiologically similar organs and tissues. This body representation is an improvement over the classical pharmacokinetic models which are based on first order transfer rates and represent the body by identifying one to three compartments based on a semilogarithmic plot of plasma concentration versus time [9]. A PBPK model uses mass-balance equations to represent the flux through a tissue compartment and the processes that take place within it. Mass balance equations can be used to ensure that the total

mass of the chemical in the body is being conserved throughout the tissue compartments. The following equation is a general mass-balance equation representing a tissue compartment.

$$V_i \frac{dC_i}{dt} = Q_i \left(C_a - \frac{C_i}{R_{i/b}} \right) \tag{2.7}$$

In Equation (2.7), i refers to tissue compartment i, V refers to volume, Q refers to the blood flow, C refers to the concentration, and $R_{i/b}$ refers to the partition coefficient between the tissue and blood [21, 29]. A partition coefficient is the ratio of the distribution of a chemical between body components at steady-state [23]. Some of the tissue compartments will have more complex mass-balance equations to represent other chemical activity within the compartment. The other chemical activities represented could be air-to-blood exchange in the lungs, metabolism in the liver, or absorption from the surface into the skin. When the system of mass-balance equations is solved simultaneously, the concentration of the chemical in each tissue compartment can be obtained, as well as, the concentration in the blood.

2.4.2 Modeling Using Dermal Subcompartments. PBPK models that identify dermal subcompartments can more accurately represent the physiology of the skin and thus improve model predictions. Subcompartment models can include biologically-based parameters which can be measured in different species and will allow extrapolation across species to be easier.

Using subcompartments in series to represent the individual layers of the skin can be more accurate than using a homogeneous skin compartment since the layers have very different permeability properties. A parallel subcompartment to represent the shunt pathway of skin appendages can also create a more accurate model since the appendages have been shown to have an effect on skin absorption.

When incorporating dermal subcompartments into a PBPK model it is necessary to created new mass-balance equations to represent the skin compartment. The new mass-balance equations introduce new parameters such as permeabilities, partition coefficients between the subcompartments, fractional areas, fractional volumes, and fractional blood flows. Some of these new parameters can be determined experimentally in the laboratory, however the unknown parameters must be estimated until measurements techniques are available. When estimating the unknown parameters, care must be taken to preserve certain relationships, for instance the permeability relationships in Equations (2.5) and (2.6). A relationship between the partition coefficients of the subcompartments and the partition coefficient of the skin must be maintained when modeling dermal subcompartments presented in Equation (2.8).

$$R_{sk/air} \cdot V_{sk} = \sum_i (R_{i/air} \cdot V_i) \qquad (2.8)$$

2.4.3 Extrapolation Across Species.   The overall goal of a PBPK model is to be able to extrapolate the results of the model across species to predict the effect of a chemical on humans [21]. The properties and methods used in interspecies extrapolation include scaling physiological parameters, physiological time, and physiologically-based pharmacokinetics. This extrapolation is not easy due to the physiological differences between laboratory animals and humans. Therefore, a PBPK model based on physiological parameters that can be measured in humans, as well as, laboratory animals can make the extrapolation process much easier [31]. In the absence of species specific parameters, body weight scaling or surface area scaling can be used. These scaling techniques depend on the characteristics of the chemical being used [42].

2.4.4 Sensitivity Analysis.   Measurement and estimation of biochemical and metabolic parameters is one reason extrapolation of model results across species is difficult. Sensitivity analysis can help determine which of the parameters are the

most important to the model's output. This will reveal which parameters should be measured or estimated most carefully [13].

There are several ways to perform sensitivity analysis on model parameters and the best method for a model depends on the information that is needed about the parameters and the model. One way to determine the sensitivity of a parameter is to observe the percent change in the model's output resulting from a certain percent change in the parameter [39]. One method of sensitivity analysis that uses this approach involves calculating a "log-normalized sensitivity coefficient". This coefficient is a ratio of the resulting percent change in the model output to the percent change in the parameter [6]. A Monte Carlo simulation using a Latin-hypercube procedure which produces estimates of the differential sensitivities of a model is sometimes used in sensitivity analysis [8].

The sensitivity of a parameter will sometimes change over time and with different exposure concentrations. Some parameters may have an inverse affect on the output of a model. That is, an increase in the parameter value will cause a decrease in the model's output. All of these considerations should be looked at before making any conclusions about the sensitivity of parameters.

2.5   A Previously Developed PBPK Model for Dermal Vapor Exposure

McDougal *et al.* (1986) developed a PBPK model for dermal absorption of vapors in the rat. Their model was developed to predict the blood concentrations of dihalomethanes after dermal exposure to chemical vapors. Figure 2.2 shows the lumped anatomical compartments of their model. This body representation was patterned after a model developed by Ramsey and Anderson (1984) which predicted the blood concentration after inhalation of styrene vapor in rats . These compartments were originally chosen because they allow the representation of metabolism and other processes that are important to the distribution of chemicals in the body. In this model, the skin is represented by a single homogeneous compartment (Fig-

2-12

ure 2.3).The following are the mass-balance equations for the body compartments of their model (Figure 2.2).
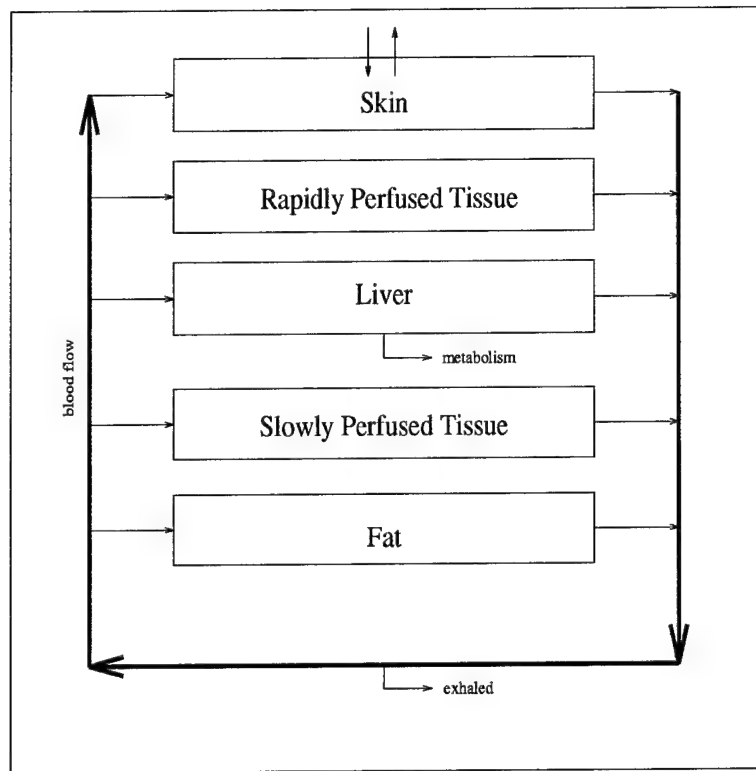
Figure 2.2   McDougal *et al.*'s Tissue Compartment Representation of the Body

Skin:

$$V_{sk}\frac{dC_{sk}}{dt} = P_{sk} \cdot A_{sk}\left(C_{sfc} - \frac{C_{sk}}{R_{sk/sfc}}\right) + Q_{sk}\left(C_a - \frac{C_{sk}}{R_{sk/b}}\right) \qquad (2.9)$$

Rapidly Perfused Tissue:

$$V_{rp}\frac{dC_{rp}}{dt} = Q_{rp}\left(C_a - \frac{C_{rp}}{R_{rp/b}}\right) \qquad (2.10)$$
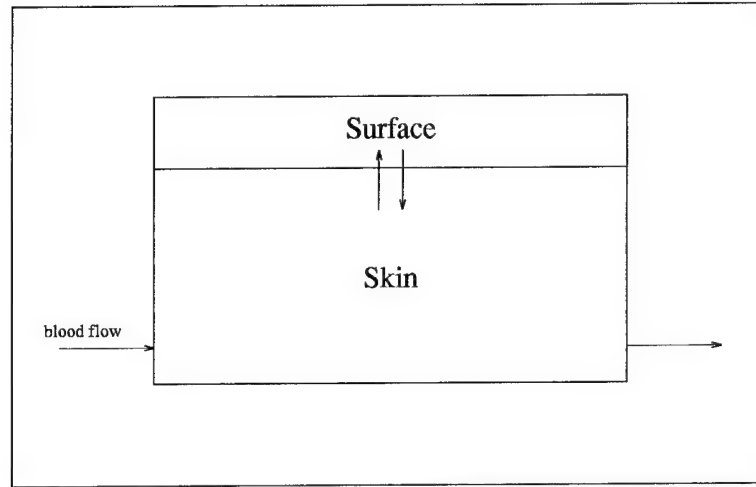
Figure 2.3   McDougal *et al.*'s Representation of the Skin Compartment

Slowly Perfused Tissue:

$$V_{sp}\frac{dC_{sp}}{dt} = Q_{sp}\left(C_a - \frac{C_{sp}}{R_{sp/b}}\right) \tag{2.11}$$

Liver:

$$V_l\frac{dC_l}{dt} = Q_l\left(C_a - \frac{C_l}{R_{l/b}}\right) - \frac{k_f \cdot C_l \cdot V_l}{R_{l/b}} - \frac{V_{max} \cdot C_l}{K \cdot R_{l/b} + C_l} \tag{2.12}$$

Fat:

$$V_f\frac{dC_f}{dt} = Q_f\left(C_a - \frac{C_f}{R_{f/b}}\right) \tag{2.13}$$

The following are the mass-balance equations their model used for the arterial blood and the venous blood returning to the lungs.

Arterial:

$$C_a = \frac{Q_c \cdot C_v}{\left(\frac{Q_{al}}{R_{b/air}} + Q_c\right)} \tag{2.14}$$

Venous:

$$C_v = \frac{\sum_i (Q_i(C_i/R_{i/b}))}{Q_c} \qquad (2.15)$$

Where:

a = arterial

A = area (distance^2)

al = alveolar

b = blood

C = concentration (mass/volume)

c = cardiac

f = fat

i = tissue compartment i

K = Michaelis constant - metabolism (mass/volume)

k_f = first-order metabolic rate constant (time^{-1})

l = liver

P = permeability (distance/time)

p = pulmonary

Q = flow (volume/time)

R = partition coefficient (ratio of concentrations)

rp = rapidly perfused

sfc = surface

sk = skin

sp = slowly perfused

t = time

V = volume

v = venous

V_{max} = maximum reaction velocity (mass/time)

The parameters for their model were obtained from the literature or measured experimentally in the laboratory and are presented in Section 4.2.1. Their model was validated for several different dihalomethanes and at several different exposure concentrations.

As opposed to using a partial differential equation, McDougal *et al.*'s model uses an ordinary differential equation to represent the diffusion equation within the context of the model. The ordinary differential equation approach assumes the skin compartment is well-stirred and thus the change in chemical concentration within the skin changes with time and not with distance through the skin. This representation of the diffusion equation allows the model to incorporate parameters that are based on biological properties (blood flow, tissue volumes, body weight, etc.) of the animal and physiochemical properties (permeability constants, partition coefficients, etc.) of the chemical being used in the model, as opposed to using multiple first-order rate constants. The advantage of using these types of parameters is that they can be measured (or optimized if absolutely necessary) in the laboratory. This allows the ability to extrapolate the results of the models to other species after appropriate parameters are measured.

2.6 *A Previously Developed Layered Dermal Subcompartment Model*

McDaniel (1993) extended the vapor model of McDougal *et al.* (1986) by adding multiple layered dermal subcompartments. His models use the same mass-balance equations as McDougal *et al.*'s vapor model except for the equation for the skin compartment (Equation (2.9)). McDaniel developed three new models that represented the skin as a series of subcompartments and compared the model predictions to experimental data.

His first model was a two subcompartment model that identified a stratum corneum subcompartment and combines the viable epidermis, dermis, and subcutaneous fat into a single composite dermal subcompartment which is where the blood exchange takes place (Figure 2.4). This model assumes the volume of the composite dermal subcompartment is the same as the volume of the stratum corneum subcompartment. Equations (2.16) and (2.17) are the new mass-balance equations for the skin subcompartment. This model made blood concentration predictions that were more accurate than the homogeneous skin model.
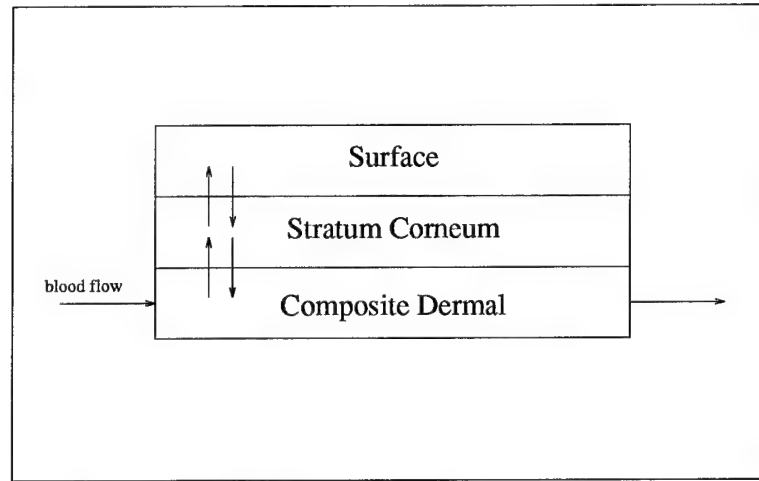
Figure 2.4   Two Layered Subcompartment Model

Stratum Corneum Subcompartment:

$$V_{sc}\frac{dC_{sc}}{dt} = P_{sc} \cdot A_{sc}\left(C_{sfc} - \frac{C_{sc}}{R_{sc/sfc}}\right) + P_{cd} \cdot A_{cd}\left(C_{cd} - \frac{C_{sc}}{R_{sc/cd}}\right) \qquad (2.16)$$

Composite Dermal Subcompartment:

$$V_{cd}\frac{dC_{cd}}{dt} = P_{cd} \cdot A_{cd}\left(\frac{C_{sc}}{R_{sc/cd}} - C_{cd}\right) + Q_{cd}\left(C_a - \frac{C_{cd}}{R_{cd/b}}\right) \qquad (2.17)$$

Where

2-17

sc = stratum corneum

cd = composite dermal

McDaniel's second model used the same equations as his first model to represent two skin subcompartments, however in the second model the volume of the composite dermal subcompartment is assumed to be ten times greater than the volume of the stratum corneum subcompartment. This model is slightly less accurate in predicting blood concentrations than the first model but is still a significant improvement over the homogeneous model, as well as, being more biologically correct.

McDaniel's third model represents the skin as three layered subcompartments. The three subcompartment model (Figure 2.5) identifies a stratum corneum subcompartment like the two subcompartment model, however the three subcompartment model breaks the composite dermal subcompartment into a viable epidermis subcompartment and a new composite dermal subcompartment consisting of the remaining layers of the skin (dermis and subcutaneous fat). The new composite dermal subcompartment is the only skin subcompartment in which blood exchange takes place. This more detailed representation improved the representation of the physiology of the skin. The volume of the viable epidermis subcompartment is assumed to be three times greater than the volume of the stratum corneum subcompartment and the volume of the new composite dermal subcompartment is assumed to be seven times greater than the volume of the stratum corneum subcompartment. This assumption preserves the size of the stratum corneum of the second two subcompartment model. The mass-balance equations for the three skin subcompartments are shown below.

Stratum Corneum Subcompartment:

$$V_{sc}\frac{dC_{sc}}{dt} = P_{sc} \cdot A_{sc}\left(C_{sfc} - \frac{C_{sc}}{R_{sc/sfc}}\right) + P_{ve} \cdot A_{ve}\left(C_{ve} - \frac{C_{sc}}{R_{sc/ve}}\right) \qquad (2.18)$$
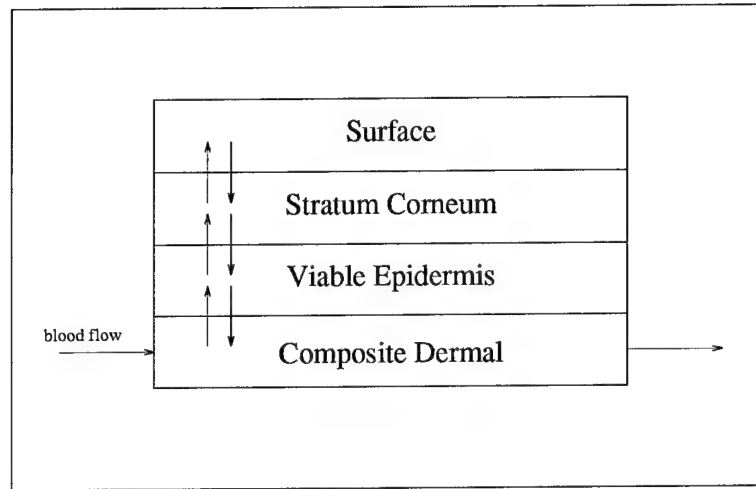
Figure 2.5   Three Layered Subcompartment Model

Viable Epidermis Subcompartment:

$$V_{ve}\frac{dC_{ve}}{dt} = P_{ve} \cdot A_{ve}\left(\frac{C_{sc}}{R_{sc/ve}} - C_{ve}\right) + P_{cd} \cdot A_{cd}\left(C_{cd} - \frac{C_{ve}}{R_{ve/cd}}\right) \qquad (2.19)$$

Composite Dermal Subcompartment:

$$V_{cd}\frac{dC_{cd}}{dt} = P_{cd} \cdot A_{cd}\left(\frac{C_{ve}}{R_{ve/cd}} - C_{cd}\right) + Q_{cd}\left(C_a - \frac{C_{cd}}{R_{cd/b}}\right) \qquad (2.20)$$

Where

ve = viable epidermis

The three subcompartment model is the most accurate of the three models for predicting blood concentrations and is the most biologically descriptive. The new models introduced several new parameters, some of which can be measured (volumes) and others which had to be optimized (permeability constants and partition coefficients). The unknown parameters were optimized by a linear search technique where the parameters were varied one at a time to determine the value which led to the smallest error between the model predictions and the experimental data. Mc-

Daniel's models were a significant improvement over the homogeneous skin model in predicting blood concentrations and in representing the physiology of the skin.

2.7 A Previously Developed PBPK Model for Dermal Neat Liquid Exposure

McDougal *et al.* developed a PBPK model to represent the absorption of a neat liquid chemical after dermal exposure. This model is similar to the vapor exposure model in that it uses the same body compartment representation (Figure 2.2). The liquid model has one additional mass-balance equation to represent the amount of the chemical on the surface of the skin (Equation (2.21)).

Amount on Skin Surface:

$$\frac{dC_{sfc}}{dt} = P_{sk} \cdot A_{sk} \left(\frac{C_{sk}}{R_{sk/lq}} - C_{sfc} \right) \tag{2.21}$$

Where

lq = Liquid

In this model the area of the skin (A_{sk}) is the area exposed to the chemical and not the entire surface area of the body as in the vapor model. The liquid model also uses different equations for the concentration in the venous blood and the concentration in the arterial blood. The vapor model assumed these blood concentrations reached steady-state so quickly compared to the concentrations in the other body compartments that the rate of change in concentration is equal to zero, thus simplifying the mass-balance equations (Equations (2.14) and (2.15)). Equations (2.22) and (2.23) are the new equations for the arterial blood concentration and the venous blood concentration.

Arterial:

$$V_a \frac{dC_a}{dt} = \left(Q_c \cdot C_v - Q_c \cdot C_a - Q_p \cdot \frac{C_a}{R_{b/air}} \right) \tag{2.22}$$

Venous:

$$V_v \frac{dC_v}{dt} = \left(\sum_i \left(Q_i \cdot \frac{C_i}{R_{i/b}} \right) \right) - (Q_c \cdot C_v) \qquad (2.23)$$

The parameters for their model were obtained from the literature or measured experimentally in the laboratory and are presented in Section 4.4.1. Their model has been validated using several chemicals by comparing the model results to experimental data collected from rats in the laboratory. This model, like the vapor model, contains biologically-based parameters that can be measured or estimated for extrapolation across species.

2.8 Summary

This review uncovered some of the complex structures and functions of the skin, as well as, some of the factors that influence the absorption of chemicals through it. The review of the previous work revealed the basic approaches used in pharmacokinetic modeling of percutaneous absorption and some of their drawbacks. A general discussion of PBPK modeling provided some of the background necessary to understand how it improves upon previous techniques of pharmacokinetic modeling. We used the background discussed in this chapter as the foundation for the new models we developed in this research.

III. Model Design and Implementation

3.1 Overview

Some Physiologically Based Pharmacokinetic (PBPK) models have been developed to predict the effect of chemicals in a rat after dermal absorption. These models are based on biological and physiological parameters that can be measured or estimated so the results can be extrapolated across species.

We have taken these previously developed models and extended them to include dermal subcompartments which represent some of the layers of the skin and the skin appendages. The dermal subcompartments give a more detailed biological description of the skin and predict blood concentrations more accurately.

3.2 Computational Methods

To solve the systems of ordinary differential mass-balance equations, we used a modified Fortran 77 program originally written by Dr. Quinn. This program solved the system of equations by calling the subroutine IVPAG from the International Mathematic and Statistics Library (IMSL). The subroutine IVPAG was created to solve an initial value problem for ordinary differential equations using an Adams-Moulton or Gear Method. We also converted some of our models to ACSL, which is the programing language the Toxicology Division of the Armstrong Laboratory uses for their skin absorption models, to ensure our method of solving the system of equations was consistent with theirs.

3.3 Optimization Technique

Our program also included a subroutine containing the method of steepest descent and Newton's Method algorithms which were used to optimize the unknown parameters to achieve the smallest weighted sum of squared deviations between the model predictions and the experimental data (Equation (3.1)) [3, 28].

$$SSD = \sum_{i=1}^{n} \left(\frac{C_{a_i(predicted)} - C_{a_i(actual)}}{weight} \right)^2 \tag{3.1}$$

Where

SSD = Sum of squared deviations

n = Number of experimental data points

The weight for each exposure was taken to be the average of all of the experimental data points for that exposure (Equation (3.2)). A weighted sum of squared deviations was used to ensure the optimization techniques did not favor a specific exposure concentration or time.

$$weight = \frac{\sum_{i=1}^{n} C_{a_i(actual)}}{n} \tag{3.2}$$

3.4 Homogeneous Vapor Model

We reconstructed McDougal *et al.*'s homogeneous vapor model presented in Section 2.5 and used it as a base to compare the predictions of the new subcompartment vapor models. The only thing that changed as we developed the subcompartment models was the equation for the skin compartment.

3.5 Layered Subcompartment Vapor Model

The layered subcompartment vapor models are based on McDaniel's models presented in Section 2.6. The layered subcompartment models used in this research have the same set of mass-balance equations as McDaniel's models. The permeability constraints of Equations (2.5) and (2.6) were included. We constrained the partition coefficients for the layered subcompartments according to Equation (2.8). Instead of the 1:10 and the 1:3:7 estimated ratios that McDaniel used, we used new measured values for the depths of the layered subcompartments. We used a stratum corneum depth of 11/560 the depth of the skin, a viable epidermis depth of 22/560 the depth

of the skin, and a composite dermal depth of 527/560 the depth of the skin [20]. Also, a conservation of mass calculations was added to ensure that all of the chemical was accounted for at all times throughout the simulation (Equation (3.3)).

$$TABS = AM_{sk} + AM_f + AM_l + AM_{sp} + AM_{rp} + AM_{ex} + AM_{met} \qquad (3.3)$$

Where

$TABS$ = Total amount absorbed (mass)

AM = Amount (mass)

ex = Exhaled

met = Metabolized

For all of the layered subcompartment models used in this research, the areas of the layered subcompartments (A_{sc}, A_{ve}, and A_{cd}) are assumed to be the same as the overall area of the skin (A_{sk}). Also, the blood flow to the composite dermal subcompartments (Q_{cd}) is assumed to be the same as the blood flow to the overall skin (Q_{sk}) because the composite dermal subcompartment is the only subcompartment in which blood exchange takes place.

3.5.1 Two Layered Subcompartment Vapor Model. The two layered subcompartment model introduced four new parameters that had to be measured or optimized. The new parameters were the stratum corneum air partition coefficient ($R_{sc/air}$), composite dermal air partition coefficient ($R_{cd/air}$), the permeability constant for the stratum corneum subcompartment (P_{sc}), and the permeability constant for the composite dermal subcompartment (P_{cd}). The permeability constant for the composite dermal subcompartment was not optimized directly because it was determined at run time by the permeability constant for the stratum corneum subcompartment through the following relationship which is based on Equation (2.5):

$$\frac{1}{P_{sk}} = \frac{1}{P_{sc}} + \frac{1}{P_{cd}} \tag{3.4}$$

Thus the equation for P_{cd} is:

$$P_{cd} = \frac{P_{sk} \cdot P_{sc}}{P_{sc} - P_{sk}} \tag{3.5}$$

The partition coefficient for the composite dermal subcompartment was not optimized directly because it was determined at run time by the partition coefficient for the stratum corneum subcompartment through the following relationship which is based on Equation (2.8):

$$R_{sk/air} \cdot V_{sk} = R_{sc/air} \cdot V_{sc} + R_{cd/air} \cdot V_{cd} \tag{3.6}$$

Thus the equation for $R_{cd/air}$ is:

$$R_{cd/air} = \frac{R_{sk/air} \cdot V_{sk} - R_{sc/air} \cdot V_{sc}}{V_{cd}} \tag{3.7}$$

Because of the uncertainty as to which subcompartment permeability and partition coefficient to optimize directly and which to optimize indirectly using Equations (3.4) and (3.6), we also optimized P_{cd} and $R_{cd/air}$ directly and allowed P_{sc} and $R_{sc/air}$ to be optimized indirectly. This process verified that the optimization procedure would produce the same results using both approaches.

3.5.2   Three Layered Subcompartment Vapor Model.   The three layered subcompartment model introduced six new parameters that had to be measured or optimized. The new parameters were the stratum corneum air partition coefficient $(R_{sc/air})$, viable epidermis air partition coefficient $(R_{ve/air})$, composite dermal air partition coefficient $(R_{cd/air})$, the permeability constant for the stratum corneum subcompartment (P_{sc}), the permeability constant for the viable epidermis subcom-

3-4

partment (P_{ve}), and the permeability constant for the composite dermal subcompartment (P_{cd}). The values of $R_{sc/air}$ and P_{sc} can be taken from the two layered subcompartment model. We could not use the value of $R_{cd/air}$ or P_{cd} from the two layered subcompartment model because the composite dermal subcompartment for the two layered subcompartment model includes the viable epidermis and the composite dermal subcompartment for the three layered subcompartment model does not. The permeability constant for the composite dermal subcompartment was not optimized directly because it was determined at run time by the permeability constant for the stratum corneum and viable epidermis subcompartments through the following relationship which is based on Equation (2.5):

$$\frac{1}{P_{sk}} = \frac{1}{P_{sc}} + \frac{1}{P_{ve}} + \frac{1}{P_{cd}} \tag{3.8}$$

Thus the equation for P_{cd} is:

$$P_{cd} = \frac{P_{sk} \cdot P_{sc} \cdot P_{ve}}{P_{sc} \cdot P_{ve} - P_{sk} \cdot P_{ve} - P_{sk} \cdot P_{sc}} \tag{3.9}$$

The partition coefficient for the composite dermal subcompartment was not optimized directly because it was determined at run time by the partition coefficients for the stratum corneum and viable epidermis subcompartments through the following relationship which is based on Equation (2.8):

$$R_{sk/air} \cdot V_{sk} = R_{sc/air} \cdot V_{sc} + R_{ve/air} \cdot V_{ve} + R_{cd/air} \cdot V_{cd} \tag{3.10}$$

Thus the equation for $R_{cd/air}$ is:

$$R_{cd/air} = \frac{R_{sk/air} \cdot V_{sk} - R_{sc/air} \cdot V_{sc} - R_{ve/air} \cdot V_{ve}}{V_{cd}} \tag{3.11}$$

As in the two layered subcompartment model, we also optimized P_{cd} and $R_{cd/air}$ directly and allowed P_{ve} and $R_{ve/air}$ to be optimized indirectly using Equations (3.8) and (3.10). This method, as opposed to the one mentioned above, verified that the optimization procedure would produce the same results using both approaches.

3.6   Parallel Subcompartment Vapor Model

We developed a parallel subcompartment vapor model to represent the shunt pathway of skin appendages through the skin. This model expanded the homogeneous vapor model by representing the skin as two parallel subcompartments (Figure 3.1). The parallel subcompartment model identifies a follicle subcompartment and a composite dermal subcompartment. The follicle subcompartment includes the hair follicles and sweat glands and the composite dermal subcompartment includes the normal layers of the skin (stratum corneum, viable epidermis, dermis, and subcutaneous fat). The composite dermal subcompartment for the parallel subcompartment model is different from the composite dermal subcompartments of the layered subcompartment models. The fractional area of the follicle subcompartment (A_{fo}) is one one-hundredth the area of the entire skin (A_{sk}) [20]. Blood exchange takes place in both subcompartments and the fractional blood flow to the follicle subcompartment (Q_{fo}) is one fourth the blood flow to the entire skin (Q_{sk}) [20]. The depth of the follicle subcompartment is assumed to be 388/560 the depth of the entire skin [20]. The following are the mass-balance equations for the two parallel subcompartments.

Follicle Subcompartment:

$$V_{fo}\frac{dC_{fo}}{dt} = P_{fo} \cdot A_{fo}\left(C_{sfc} - \frac{C_{fo}}{R_{fo/sfc}}\right) + Q_{fo}\left(C_a - \frac{C_{fo}}{R_{fo/b}}\right) \qquad (3.12)$$
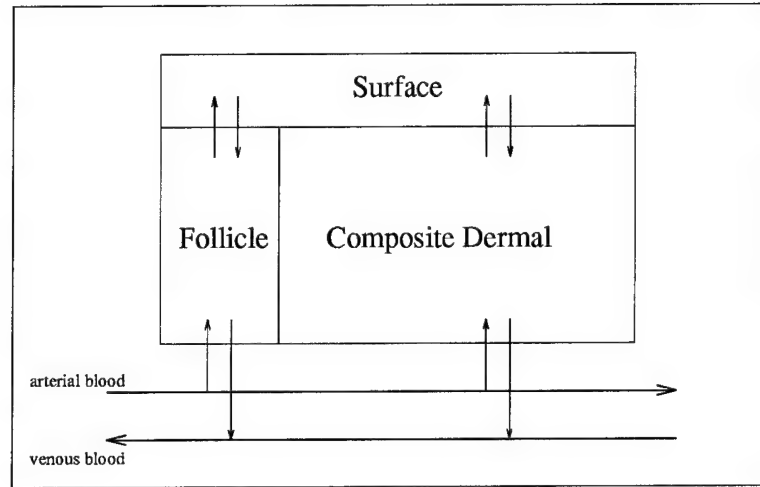
Figure 3.1   Parallel Subcompartment Vapor Model

Composite Dermal Subcompartment:

$$V_{cd}\frac{dC_{cd}}{dt} = P_{cd} \cdot A_{cd}\left(C_{sfc} - \frac{C_{cd}}{R_{cd/sfc}}\right) + Q_{cd}\left(C_a - \frac{C_{cd}}{R_{cd/b}}\right) \qquad (3.13)$$

Where

fo = Follicle

Equations (3.12) and (3.13) replace Equation (2.9) in the homogeneous model. The parallel subcompartment model introduced four new parameters that had to be measured or optimized. The new parameters are the follicle air partition coefficient ($R_{fo/air}$), the composite dermal air partition coefficient ($R_{cd/air}$), the follicle permeability constant (P_{fo}), and the composite dermal permeability constant (P_{cd}). The permeability constant for the composite dermal subcompartment was not optimized directly because it was determined at run time by the permeability constant for the follicle subcompartment through the following relationship which is an application of Equation (2.6):

$$P_{sk} \cdot A_{sk} = P_{fo} \cdot A_{fo} + P_{cd} \cdot A_{cd} \qquad (3.14)$$

3-7

Thus the equation for P_{cd} is:

$$P_{cd} = \frac{P_{sk} \cdot A_{sk} - P_{fo} \cdot A_{fo}}{A_{cd}} \qquad (3.15)$$

The partition coefficient for the composite dermal subcompartment was not optimized directly because it was determined at run time by the partition coefficient for the follicle subcompartment through the following relationship which is based on Equation (2.8):

$$R_{sk/air} \cdot V_{sk} = R_{fo/air} \cdot V_{fo} + R_{cd/air} \cdot V_{cd} \qquad (3.16)$$

Thus the equation for $R_{cd/air}$ is:

$$R_{cd/air} = \frac{R_{sk/air} \cdot V_{sk} - R_{fo/air} \cdot V_{fo}}{V_{cd}} \qquad (3.17)$$

As in the layered subcompartment models, we also optimized P_{cd} and $R_{cd/air}$ directly and allowed P_{fo} and $R_{fo/air}$ to be optimized indirectly using Equations (3.14) and (3.16). This method, as opposed to the one mentioned above, verified that the optimization procedure would produce the same results using both approaches.

3.7 Parallel-Layered Subcompartment Vapor Model

We developed a new model that combined the two layered subcompartment model and the parallel subcompartment model. This new parallel-layered subcompartment model expanded the homogeneous vapor model by representing the skin as three subcompartments which are the follicle, stratum corneum and the composite dermal (Figure 3.2). The follicle subcompartment includes the hair follicles and sweat glands. The stratum corneum subcompartment consists of the stratum corneum and the composite dermal subcompartment includes the remaining layers of the skin (viable epidermis, dermis, and subcutaneous fat). The composite dermal

subcompartment for the parallel-layered subcompartment model is different from the previously discussed composite dermal subcompartments. The fractional area of the follicle subcompartment (A_{fo}) is one one-hundredth the area of the entire skin (A_{sk}) [20]. Blood exchange takes place in both subcompartments and the fractional blood flow to the follicle subcompartment (Q_{fo}) is one fourth the blood flow to the entire skin (Q_{sk}) [20]. The depth of the follicle subcompartment is assumed to be $388/560$ the depth of the entire skin [20]. The depth of the composite dermal subcompartment is assumed to be $549/560$ the depth of the entire skin. The areas of the layered subcompartments $(A_{sc}$ and $A_{cd})$ are assumed to be the same as the overall area of the non-follicle portion of the skin $(A_{cd}$ from the parallel subcompartment model). Also, the blood flow to the composite dermal subcompartments (Q_{cd}) is assumed to be the same as the blood flow to the overall non-follicle portion of the skin $(Q_{cd}$ from the parallel subcompartment model) because the composite dermal subcompartment is the only layered subcompartment in which blood exchange takes place. The following are the mass-balance equations for the three skin subcompartments of the parallel-layered subcompartment model.
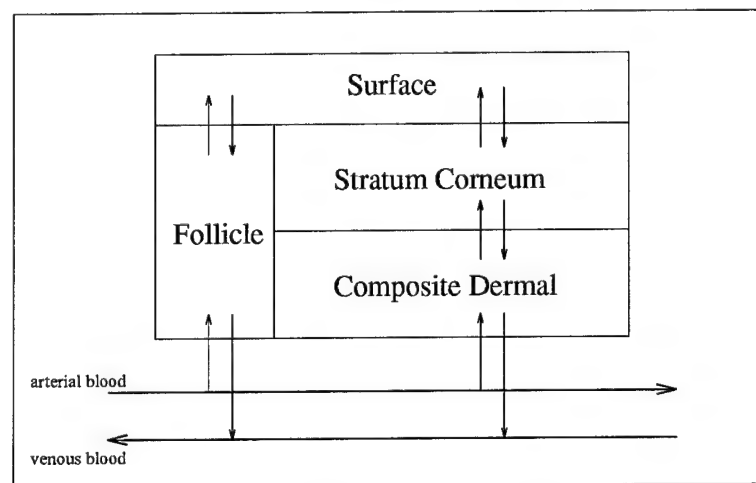
Figure 3.2   Parallel-Layered Subcompartment Model

Follicle Subcompartment:

$$V_{fo}\frac{dC_{fo}}{dt} = P_{fo} \cdot A_{fo}\left(C_{sfc} - \frac{C_{fo}}{R_{fo/sfc}}\right) + Q_{fo}\left(C_a - \frac{C_{fo}}{R_{fo/b}}\right) \qquad (3.18)$$

Stratum Corneum Subcompartment:

$$V_{sc}\frac{dC_{sc}}{dt} = P_{sc} \cdot A_{sc}\left(C_{sfc} - \frac{C_{sc}}{R_{sc/sfc}}\right) + P_{cd} \cdot A_{cd}\left(C_{cd} - \frac{C_{sc}}{R_{sc/cd}}\right) \qquad (3.19)$$

Composite Dermal Subcompartment:

$$V_{cd}\frac{dC_{cd}}{dt} = P_{cd} \cdot A_{cd}\left(\frac{C_{sc}}{R_{sc/cd}} - C_{cd}\right) + Q_{cd}\left(C_a - \frac{C_{cd}}{R_{cd/b}}\right) \qquad (3.20)$$

Equations (3.18), (3.19), and (3.20) replace Equation (2.9) in the homogeneous model. The parallel-layered subcompartment model introduced six new parameters that had to be measured or optimized. The new parameters are the follicle air partition coefficient ($R_{fo/air}$), the stratum corneum air partition coefficient ($R_{sc/air}$), the composite dermal air partition coefficient ($R_{cd/air}$), the follicle permeability constant (P_{fo}), the stratum corneum permeability constant (P_{sc}), and the composite dermal permeability constant (P_{cd}). The value of $R_{fo/air}$ and P_{fo} were taken from the parallel subcompartment model since the follicle subcompartment is physiologically the same for both models. The parameters for the stratum corneum subcompartment and the composite dermal subcompartment had to be optimized because these subcompartments are different from the ones in the two layered subcompartment model because in this model they do not include the follicle region of the skin. The permeability constant for the composite dermal subcompartment was not optimized directly because it was determined at run time by the permeability constant for the stratum corneum subcompartment through the following relationship which is an application of Equations (2.5) and (2.6).

$$P_{sk} \cdot A_{sk} = P_{fo} \cdot A_{fo} + \left(\frac{1}{P_{sc}} + \frac{1}{P_{cd(Fig\ 3.2)}} \right)^{-1} \cdot A_{cd} \qquad (3.21)$$

Notice that Equation (3.21) is the same as Equation (3.14) except that

$$P_{cd(Fig\ 3.1)} = \left(\frac{1}{P_{sc}} + \frac{1}{P_{cd(Fig\ 3.2)}} \right)^{-1} \qquad (3.22)$$

where $cd(Fig\ 3.1)$ is the composite dermal subcompartment of Figure 3.1 and $cd(Fig\ 3.2)$ is the composite dermal subcompartment of Figure 3.2. Thus the equation for $P_{cd(Fig\ 3.2)}$ is:

$$P_{cd(Fig\ 3.2)} = \frac{P_{sc} \cdot P_{sk} \cdot A_{sk} - P_{sc} \cdot P_{fo} \cdot A_{fo}}{P_{sc} \cdot A_{cd} - P_{sk} \cdot A_{sk} + P_{fo} \cdot A_{fo}} \qquad (3.23)$$

The partition coefficient for the composite dermal subcompartment was not optimized directly because it was determined at run time by the partition coefficients for the stratum corneum and follicle subcompartments through the following relationship which is based on Equation (2.8):

$$R_{sk/air} \cdot V_{sk} = R_{sc/air} \cdot V_{sc} + R_{cd/air} \cdot V_{cd} + R_{fo/air} \cdot V_{fo} \qquad (3.24)$$

Thus the equation for $R_{cd/air}$ is:

$$R_{cd/air} = \frac{R_{sk/air} \cdot V_{sk} - R_{sc/air} \cdot V_{sc} - R_{fo/air} \cdot V_{fo}}{V_{cd}} \qquad (3.25)$$

We also optimized P_{cd} and $R_{cd/air}$ directly and allowed P_{sc} and $R_{sc/air}$ to be optimized indirectly using Equations (3.21) and (3.24). This method, as opposed to the one mentioned above, verified that the optimization procedure would produce the same results using both approaches.

3.8 Homogeneous Liquid Model

We reconstructed McDougal *et al.*'s homogeneous liquid model presented in Section 2.7 and used it as a base to compare the predictions of the subcompartment liquid models. The mass-balance equations for these subcompartment models are the same as the ones in McDougal *et al.*'s model except for the equation for the skin compartment.

3.9 Liquid Subcompartment Models

We used the same approach as we did with the homogeneous vapor model to develop four new liquid subcompartment models (two layered subcompartment model, three layered subcompartment model, parallel subcompartment model, and parallel-layered subcompartment model). The equations for the skin subcompartments in each liquid subcompartment model are almost the same as the ones in the corresponding vapor subcompartment models. The only difference is that in the liquid models we use subcompartment liquid partition coefficients instead of subcompartment surface partition coefficients.

3.10 Sensitivity Analysis

It is important to know which parameters have the largest effect on the models' blood concentration predictions. We performed sensitivity analysis to identify the skin compartment parameters that cause the largest percent change in arterial blood concentration predictions when they are changed by a set percent from their original values. One at a time, we increased and decreased the values of the parameters by five percent and computed blood concentration profiles. We chose a time early in the exposure and a time late in the exposure and determined the amount the output changed due to a five percent change in the parameters.

3.11 Summary

We have taken the previously developed homogeneous models and extended them to include dermal subcompartments in series to represent the layers of the skin and in parallel to represent the skin appendages. Although the new parameters are biologically based, some of them had to be estimated until better measurement techniques are developed in the laboratory. The new subcompartment models predict blood concentrations more accurately because they provide a better biological description of the skin and they have more parameters that are optimized.

IV. Model Results

4.1 Overview

The predictions of the new models were compared to experimental data in which rats were exposed certain chemicals for specified periods of time which the models are set up to simulate. The sum of squared deviations and graphical plots are used to measure how well the models' predictions match the experimental data. The subcompartment models' results were compared to the homogeneous models' results to ensure the new subcompartment models were at least as accurate as the original models. Sensitivity analysis performed on the skin compartment parameters in the models showed which of the parameters have the largest effect on the predicted arterial blood concentrations of the chemicals.

4.2 Vapor Model Predictions

The blood concentration predictions from the five vapor models were compared to previously collected data in which rats were exposed to dibromomethane (DBM) vapor at concentrations of 500 ppm, 1,000 ppm, 5,000 ppm, and 10,000 ppm for four hour periods [22]. The increase in accuracy from the homogeneous model to the subcompartment models may not be immediately obvious since the graphs are displayed with a logarithmic scale and the relative differences between the actual data and the predictions are already small.

4.2.1 Homogeneous Vapor Model. The parameters for the homogeneous model were determined experimentally or found in the literature (Tables 4.1 and 4.2) [23]. Figure 4.1 shows how the predictions of the previously published homogeneous model compare to the experimental data. The homogeneous model predicted the concentrations in the blood reasonably well having a sum of squared deviations of 0.55 when compared to the experimental data.

4-1

Compartment	Tissue/air partition coefficient	Blood flow (% cardiac output)	Volume (% body weight)
Skin	266.0	5	10
Rapidly Perfused	68.1	56	5
Slowly Perfused	40.5	10	65
Fat	792.0	9	7
Liver	68.1	20	4
Blood	74.1	N/A	N/A

Table 4.1   DBM Parameters for the tissue compartments of the homogenous vapor model

Constants	Values
V_{max} (mg/hr/kg)	12.5
K_m (mg/liter)	0.4
K_f (hr^{-1}·kg^{-1})	3.4
K_p (cm/hr)	1.32

Table 4.2   DBM Constants for the homogenous vapor model

4.2.2   Two Layered Subcompartment Vapor Model.   The unknown subcompartment permeability constants and partition coefficients of the two layered subcompartment model were estimated and the optimized parameter values can be seen in Table 4.3. The two layered subcompartment model matched the data better than the homogeneous model, yielding a sum of squared deviations of 0.40 when compared to the experimental data. The two layered subcompartment model's sum of squared deviations is a 27 percent improvement in accuracy over the homogeneous model. Figure 4.2 shows how well the predicted values of the two layered subcompartment model match the experimental data. The two layered subcompartment model predicts the concentration of the chemical in the blood more accurately than the homogeneous model, because it is a more physiologically detailed representation of the skin and it has two more parameters that were optimized.

4-2

Figure 4.1   DBM Homogeneous Vapor Model Results. This graph shows how the model's predictions compare to the experimental data.

Unknown Parameters	Optimized Values
P_{sc}	1.46
P_{cd}	14.00
$R_{sc/air}$	1530.52
$R_{cd/air}$	240.66
Sum of Squared Deviations	0.40

Table 4.3   DBM Two Layered Subcompartment Vapor Model Estimated Parameters

Figure 4.2   DBM Two Layered Subcompartment Vapor Model Results. This graph
shows how the model's predictions compare to the experimental data.

4.2.3   Three Layered Subcompartment Vapor Model.   The unknown sub-
compartment permeability constants and partition coefficients of the three layered
subcompartment model were estimated and the optimized parameter values can be
seen in Table 4.4.   The three layered subcompartment model yielded about the
same results as the two layered subcompartment model yielding a sum of squared
deviations of 0.40 when compared to the experimental data. The three layered sub-
compartment model's sum of squared deviations is a 27 percent improvement in
accuracy over the homogeneous model.   Figure 4.3 shows how well the predicted
concentration values of the three layered subcompartment model match the experi-
mental data. The three layered subcompartment model yields more accurate blood
concentration predictions, as well as, a more detailed representation of the structure
of the skin.

Unknown Parameters	Optimized Values
P_{sc}	1.46
P_{ve}	17.47
P_{cd}	70.36
$R_{sc/air}$	1530.53
$R_{ve/air}$	351.12
$R_{cd/air}$	236.05
Sum of Squared Deviations	0.40

Table 4.4 DBM Three Layered Subcompartment Vapor Model Estimated Parameters

Figure 4.3 DBM Three Layered Subcompartment Vapor Model Results. This graph shows how the model's predictions compare to the experimental data.

4.2.4 Parallel Subcompartment Vapor Model. The unknown subcompartment permeability constants and partition coefficients of the parallel subcompartment model were estimated and the optimized parameter values can be seen in Table 4.5. The parallel subcompartment model made better predictions than the homogeneous model and the layered subcompartment models. The parallel subcompartment model resulted in a sum of squared deviations of 0.37 which is a 33 percent improvement over the homogeneous model. Figure 4.4 shows how well the predicted blood concentration values of the parallel subcompartment model match the experimental data.

Unknown Parameters	Optimized Values
P_{fo}	94.04
P_{cd}	0.38
$R_{fo/air}$	325.08
$R_{cd/air}$	265.59
Sum of Squared Deviations	0.37

Table 4.5   DBM Parallel Subcompartment Vapor Model Estimated Parameters

4.2.5 Parallel-Layered Subcompartment Vapor Model. The unknown subcompartment permeability constants and partition coefficients of the parallel-layered subcompartment model were estimated and the optimized parameter values can be seen in Table 4.6. The parallel-layered subcompartment model made better blood concentration predictions than the homogeneous model, the layered subcompartment models, and the parallel subcompartment model. The parallel-layered subcompartment model resulted in a sum of squared deviations of 0.30 which is a 45 percent improvement over the homogeneous model. Figure 4.5 shows how well the predicted concentration values of the parallel-layered subcompartment model match the experimental data.
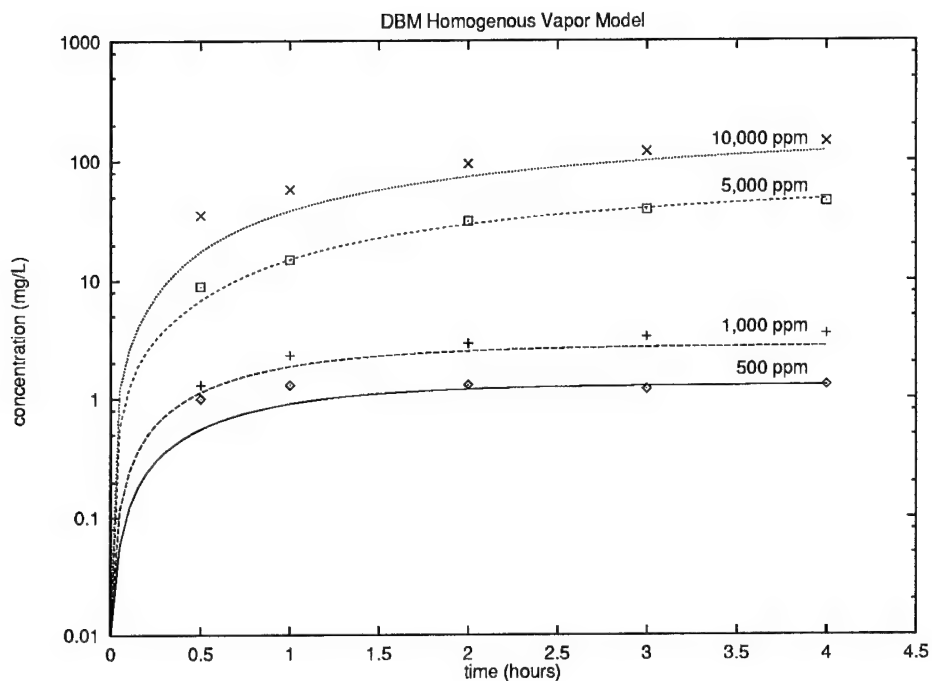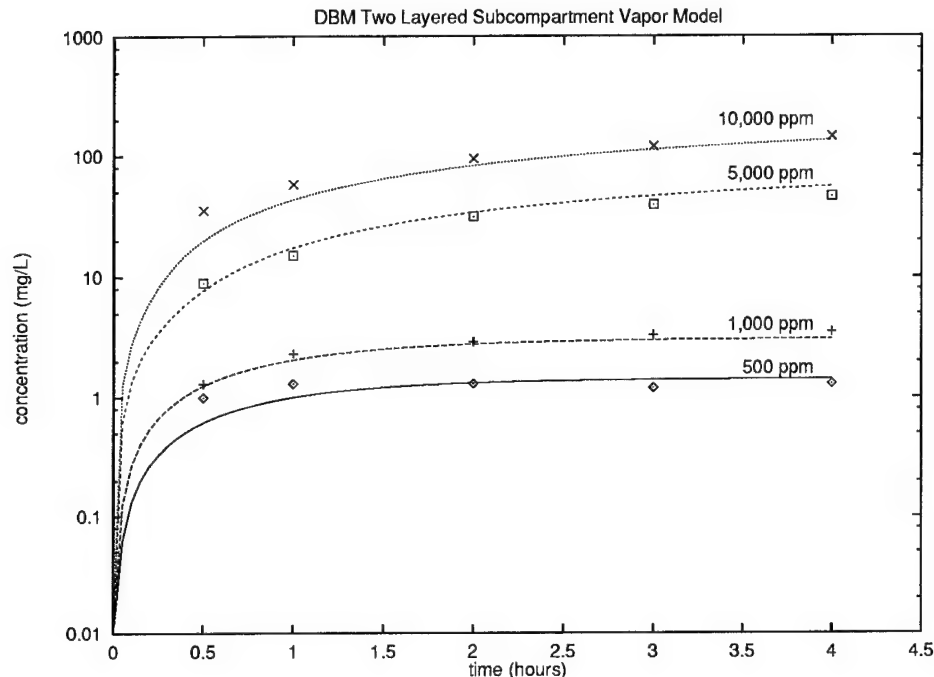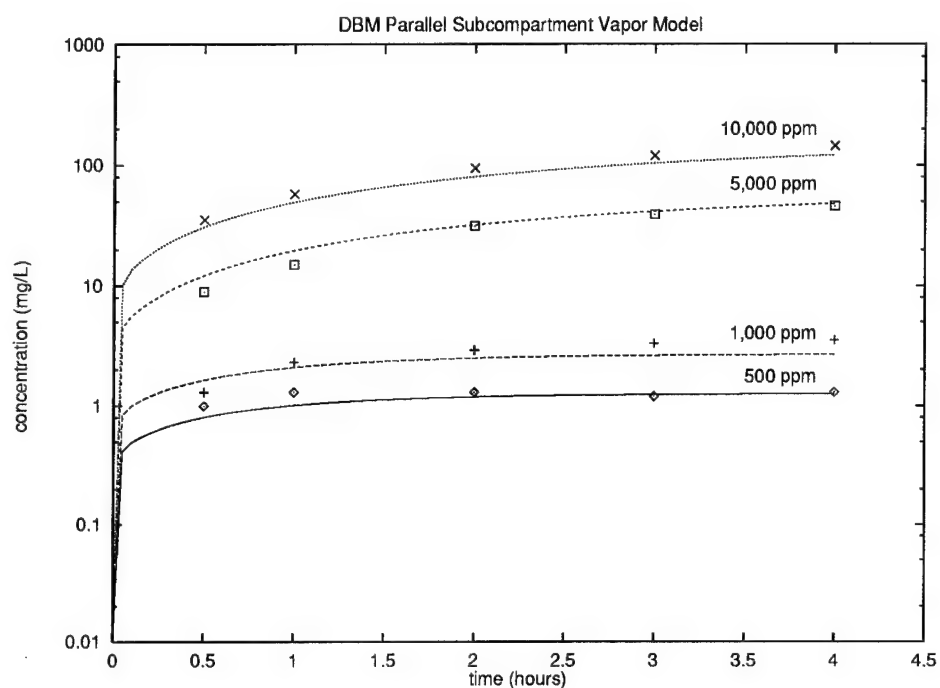
Figure 4.4   DBM Parallel Subcompartment Vapor Model Results. This graph shows
how the model's predictions compare to the experimental data.

Unknown Parameters	Optimized Values
P_{fo}	94.04
P_{sc}	0.46
P_{cd}	2.28
$R_{fo/air}$	325.08
$R_{sc/air}$	649.15
$R_{cd/air}$	257.93
Sum of Squared Deviations	0.30

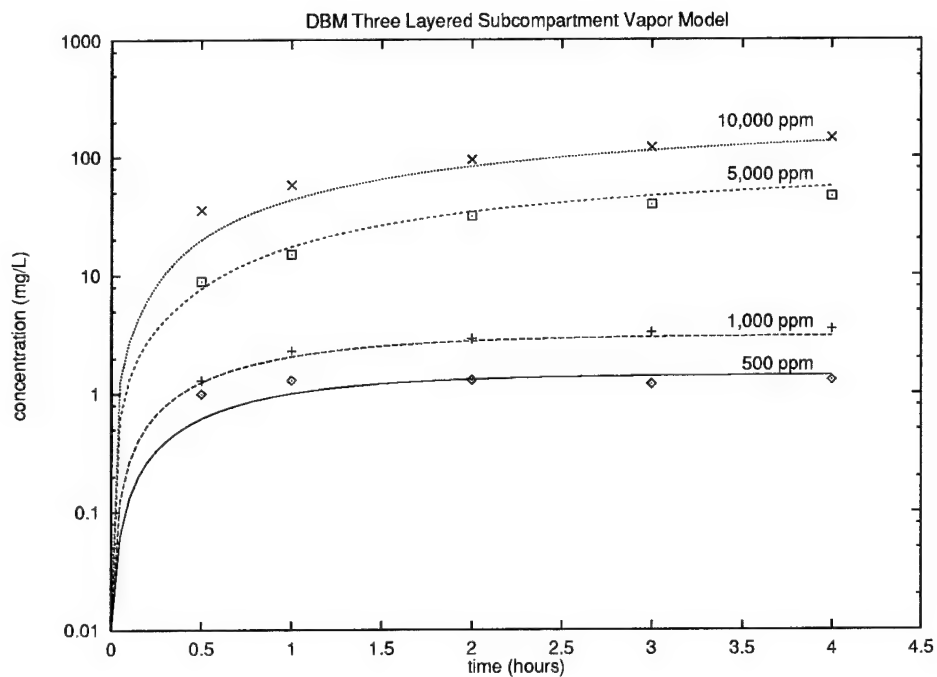Table 4.6   DBM   Parallel-Layered   Subcompartment   Vapor   Model   Estimated
Parameters

4-7
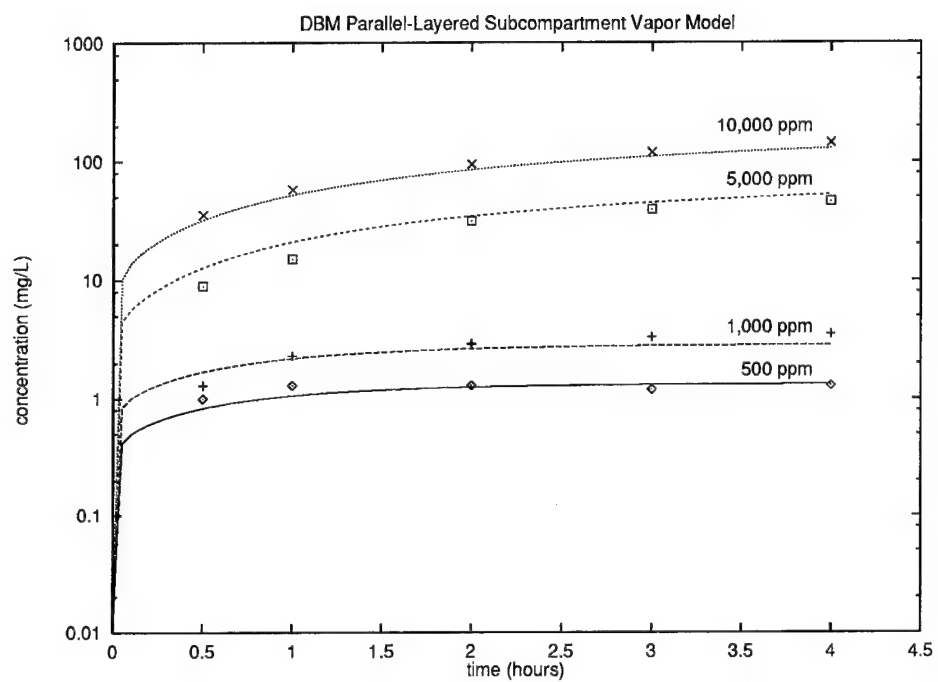
Figure 4.5 DBM Parallel-Layered Subcompartment Vapor Model Results. This graph shows how the model's predictions compare to the experimental data.

4.3 Sensitivity Analysis for Vapor Models

We conducted sensitivity analysis on the parameters of the skin compartments of each model to determine the impact they had on the predicted blood concentration (Tables 4.7–4.11). We looked at the percent change in predicted blood concentrations at one-half hour and at four hours for each change in the parameters for the 500 ppm and 10,000 ppm exposures. In each of the models, the predicted blood concentration was the most sensitive to changes in one of the subcompartment permeability constants. The blood concentration predictions were much less sensitive to the parameters of the mass-balance equations for body compartments other than the skin. The most sensitive parameters in the other body compartments were blood flow to the liver (Q_l), fat blood partition coefficient ($R_{f/b}$), volume of the fat compartment (V_f), and blood flow to the fat compartment (Q_f), in that order (data not shown). Increasing the parameters by five percent had relatively the same effect as decreasing the parameter by five percent, although the direction was different. The rest of this discussion will pertain to the effect of increasing the parameters by five percent. Most of the parameters had a greater sensitivity at the higher concentration than they did at the lower concentration because metabolism is saturated at the higher concentration and the increase of chemical into the body is more directly reflected in predicted blood concentration.

4.3.1 Homogeneous Vapor Model. In the homogeneous model, the order of sensitivity was permeability (P), blood air partition coefficient ($R_{b/air}$), skin air partition coefficient ($R_{sk/air}$), and flow to the skin (Q_{sk}) (Table 4.7). Increasing the most sensitive parameter, permeability, increased the predicted blood concentration by nearly equivalent percentages during a one-half hour exposure and during a four-hour exposure. Changes in the blood air and skin air partition coefficients and the blood flow to the skin had much more effect on predicted blood concentrations after one-half hour than after four hours, because early in the exposure the concentration difference between skin and the environment is much greater than after four hours.

4-9

| | 500 ppm | | 10,000 ppm | |
Parameter	.5 hours +5%	4 hours +5%	.5 hours +5%	4 hours +5%
P	5.0	5.0	6.4	5.8
$R_{b/air}$	3.3	0.5	4.6	2.6
$R_{sk/air}$	-3.1	-0.1	-4.1	-1.0
Q_{sk}	2.7	0.2	3.5	0.5

Table 4.7   Sensitivity Analysis for the DBM Homogenous Vapor Model. These numbers represent the percent change in predicted blood concentrations after the parameters were varied.

4.3.2   Two Layered Subcompartment Vapor Model.   In the two layered subcompartment model, changing the permeability for stratum corneum (P_{sc}) had the largest impact on the predicted blood concentration while the composite dermal permeability (P_{cd}) had practically no effect (Table 4.8). This is because P_{cd} is so large compared to P_{sc} that a five percent change in P_{cd} resulted in a very small change in the overall permeability of the skin from Equation (3.4), but a five percent change in P_{sc} resulted in about a five percent change in the overall permeability. In contrast, the predicted blood concentration was much more sensitive to changes in the composite dermal partition coefficient $(R_{cd/air})$ than it was to changes in the stratum corneum partition coefficient $(R_{sc/air})$. It is interesting to note that in this model the volume of the composite dermal subcompartment is about fifty times that of the stratum corneum subcompartment and the value for the stratum corneum air partition coefficient is almost one order of magnitude greater than the optimized value of the composite dermal air partition coefficient. In this model, the partition coefficients and the flow to the skin (Q_{sk}) had more impact on the blood concentration after one-half hour than after four hours, because the concentration difference between air and skin was diminished after four hours.

4.3.3   Three Layered Subcompartment Vapor Model.   In the three layered subcompartment model, like the two layered subcompartment model, changing the

4-10

Parameter	500 ppm		10,000 ppm	
	.5 hours +5%	4 hours +5%	.5 hours +5%	4 hours +5%
P_{sc}	5.0	5.0	6.3	5.7
$R_{b/air}$	3.3	0.6	4.6	2.6
$R_{cd/air}$	-2.7	-0.1	-3.6	-0.9
Q_{sk}	2.7	0.2	3.4	0.5
$R_{sc/air}$	-0.4	0.0	-0.5	-0.1
P_{cd}	0.0	0.0	0.0	0.0

Table 4.8   Sensitivity Analysis for the DBM Two Layerd Subcompartment Vapor Model. These numbers represent the percent change in predicted blood concentrations after the parameters were varied.

permeability for stratum corneum (P_{sc}) had a much larger impact on the predicted blood concentration than the permeability of the viable epidermis (P_{ve}) and the composite dermal (P_{cd}) (Table 4.9). When these parameters were estimated, the composite dermal and the viable epidermis permeabilities were significantly larger than the stratum corneum permeability. This caused a five percent change in P_{cd} and P_{ve} to change the overall permeability of the skin by only a small percent through Equation (3.8) which resulted in a low sensitivity for P_{cd} and P_{ve}. Skin subcompartment air partition coefficients had an order of sensitivity of composite dermal $(R_{cd/air})$, stratum corneum $(R_{sc/air})$, and then viable epidermis $(R_{ve/air})$. The composite dermal was quite a bit more sensitive. It appears that the partition coefficient for the composite dermal subcompartment had the most effect on chemical transport through the rest of the skin.

4.3.4   Parallel Subcompartment Vapor Model.   In the parallel subcompartment model, changing the permeability of the follicle subcompartment (P_{fo}) had the largest effect on the predicted blood concentrations (Table 4.10). The blood air partition coefficient $(R_{b/air})$ had the next largest impact which is consistent with the layered subcompartment models. The permeability of the composite dermal subcom-

| | 500 ppm | | 10,000 ppm | |
| | .5 hours | 4 hours | .5 hours | 4 hours |
Parameter	+5%	+5%	+5%	+5%
P_{sc}	5.0	5.0	6.3	5.7
$R_{b/air}$	3.4	0.6	4.6	2.6
$R_{cd/air}$	-2.6	-0.1	-3.4	-0.9
Q_{sk}	2.7	0.2	3.4	0.5
$R_{sc/air}$	-0.3	-0.0	-0.5	-0.1
$R_{ve/air}$	-0.2	0.0	-0.2	-0.1
P_{ve}	0.0	0.0	0.0	0.0
P_{cd}	0.0	0.0	0.0	0.0

Table 4.9   Sensitivity Analysis for the DBM Three Layered Subcompartment Vapor Model. These numbers represent the percent change in predicted blood concentrations after the parameters were varied.

partment (P_{cd}) had the next largest impact which was probably because it contains the stratum corneum. The composite dermal air partition coefficient ($R_{cd/air}$) was more sensitive than the follicle air partition coefficient ($R_{fo/air}$) which was probably due to the small fractional area of the follicle subcompartment (10^{-2}). The flow to the follicle (Q_{fo}) and composite dermal (Q_{cd}) subcompartments was much less sensitive than the flow to the skin (Q_{sk}) in the layered subcompartment models.

4.3.5   Parallel-Layered Subcompartment Vapor Model.   In the parallel-layered subcompartment model, like in the parallel subcompartment model, changing the permeability of the follicle subcompartment (P_{fo}) had the largest effect on the predicted blood concentrations (Table 4.11). After the blood air partition coefficient ($R_{b/air}$), the permeability of the stratum corneum subcompartment (P_{sc}) had the next largest effect on the blood concentration predictions. Since the permeability of the composite dermal subcompartment (P_{cd}) is relatively large compared to P_{sc}, changing P_{cd} by five percent actually changed the overall permeability of the non-follicle skin subcompartment by a very small percent because of Equation (3.21). The stratum corneum air partition coefficient ($R_{sc/air}$) had relatively no impact when

Parameter	500 ppm		10,000 ppm	
	.5 hours +5%	4 hours +5%	.5 hours +5%	4 hours +5%
P_{fo}	3.9	3.4	4.9	4.0
$R_{b/air}$	1.3	0.7	1.8	2.6
P_{cd}	0.9	1.5	0.9	1.7
$R_{cd/air}$	-0.7	-0.1	-0.9	-0.8
Q_{fo}	0.3	0.2	0.4	0.3
Q_{cd}	0.4	0.1	0.2	0.2
$R_{fo/air}$	0.0	0.0	-0.1	0.0

Table 4.10 Sensitivity Analysis for the DBM Parallel Subcompartment Vapor Model. These numbers represent the percent change in predicted blood concentrations after the parameters were varied.

varied which is consistent with the layered subcompartment models. The remaining parameters had the same order of sensitivity and relatively the same magnitudes of sensitivity as in the parallel subcompartment model.

4.4 Liquid Model Predictions

The blood concentration predictions from the five liquid models were compared to previously collected data in which rats were exposed to neat dibromomethane (DBM) liquid in a cell with an area of 3.14 cm at a dose of 7434 ppm for a twenty four hour period [16]. Although the liquid and vapor models both use dibromomethane (DBM), they should not be compared because of the differences in some of the parameter values for DBM. These parameter differences are a result of different researchers measuring the parameters and a ten year gap in the development of the models.

The subcompartment models were optimized using the technique described in Section 3.3, however we weighted the last data point very low (100 times lower) compared to the first seven data points. We did this so the optimization technique would focus on the early data points since those are the times we are most interested

| | 500 ppm | | 10,000 ppm | |
| | .5 hours | 4 hours | .5 hours | 4 hours |
Parameter	+5%	+5%	+5%	+5%
P_{fo}	3.8	3.2	4.7	3.7
$R_{b/air}$	1.3	0.7	1.9	2.6
P_{sc}	1.0	1.7	1.1	1.9
$R_{cd/air}$	-0.8	-0.1	-1.0	-0.8
Q_{fo}	0.3	0.2	0.4	0.2
Q_{cd}	0.5	0.1	0.3	0.2
$R_{fo/air}$	0.2	0.2	0.3	0.3
$R_{sc/air}$	0.0	0.0	-0.1	0.0
P_{cd}	0.0	0.0	0.0	0.0

Table 4.11 Sensitivity Analysis for the DBM Parallel-Layered Subcompartment Vapor Model. These numbers represent the percent change in predicted blood concentrations after the parameters were varied.

in. Also, we are not sure if the chemical physically changes the skin after a long exposure. Figures 4.6–4.10 show how each model compares to the experimental data individually and Figure 4.11 shows all five of the liquid models on the same graph to illustrate the relative improvements.

4.4.1 Homogeneous Liquid Model.   The homogeneous liquid model skin compartment is set up to represent the stratum corneum only, as opposed to the homogeneous vapor model which has a skin compartment representing the whole skin. The parameters in the homogeneous liquid model present a relatively thin skin compartment with the properties of the upper layer of the skin.

The parameters for the homogeneous model were determined experimentally or found in the literature (Tables 4.12 and 4.13) [16]. It should be noted that the permeability of the skin in this model was optimized using an equal weight on all of the data points ($P_{sk} = .003$). We also optimized the permeability using the same technique that was used for optimizing parameters in the subcompartment models (lower weight on the last data point) and obtained a different permeability

4-14

$(P_{sk} = .0032)$. Figure 4.6 shows how the predictions of the previously developed homogeneous model compare to the experimental data using both values for the permeability. For the two layered subcompartment model, we used the original permeability $(P_{sk} = .003)$ as the permeability of the stratum corneum and after optimizing the permeability of the composite dermal subcompartment, we calculated the overall skin permeability using Equation (3.4) which we then used for the other subcompartment models. For this reason, we will compare the subcompartment models to the original homogeneous model which uses $P_{sk} = .003$. The original homogeneous model predicted the concentrations in the blood reasonably well having a sum of squared deviations of 0.098 when compared to the experimental data.

Compartment	Tissue/air partition coefficient	Blood flow (% cardiac output)	Volume (% body weight)
Skin	120.00	5	10
Rapidly Perfused	0.9	56	5
Slowly Perfused	0.546	10	65
Fat	10.8	9	7
Liver	0.918	20	4
Blood	74.1	N/A	N/A

Table 4.12   DBM Parameters for the tissue compartments of the homogenous liquid model

Constants	Values
V_{max} (mg/hr/kg)	12.5
K_m (mg/liter)	.36
K_f (hr^{-1}·kg^{-1})	.557
K_p (cm/hr)	0.003

Table 4.13   DBM Constants for the homogenous liquid model

4.4.2   Two Layered Subcompartment Liquid Model.   The unknown subcompartment permeability constants and partition coefficients of the two layered

Figure 4.6   DBM Homogeneous Liquid Model Results. This graph shows how the model's predictions compare to the experimental data.

subcompartment model were estimated and the optimized parameter values can be seen in Table 4.14. The two layered subcompartment model matched the data better than the homogeneous model, yielding a sum of squared deviations of 0.063 when compared to the experimental data. The two layered subcompartment model's sum of squared deviations is a 36 percent improvement in accuracy over the homogeneous model. Figure 4.7 shows how well the predicted values of the two layered subcompartment model match the experimental data. The two layered subcompartment model predicts the concentration of the chemical in the blood more accurately than the homogeneous model, because it is a more physiologically detailed representation of the skin and it has one more parameters that was optimized.

4.4.3   Three Layered Subcompartment Liquid Model.   The unknown subcompartment permeability constants and partition coefficients of the three layered subcompartment model were estimated and the optimized parameter values can

Unknown Parameters	Optimized Values
P_{sc}	0.003
P_{cd}	5.00
$R_{sc/air}$	120.00
$R_{cd/air}$	66.96
Sum of Squared Deviations	0.063

Table 4.14   DBM Two Layered Subcompartment Liquid Model Estimated Parameters

Figure 4.7   DBM Two Layered Subcompartment Liquid Model Results. This graph shows how the model's predictions compare to the experimental data.

4-17

be seen in Table 4.15. The three layered subcompartment model yielded about the same results as the two layered subcompartment model resulting in a sum of squared deviations of 0.060 when compared to the experimental data. The three layered subcompartment model's sum of squared deviations is a 39 percent improvement in accuracy over the homogeneous model. Figure 4.8 shows how well the predicted concentration values of the three layered subcompartment model match the experimental data. The three layered subcompartment model yields more accurate blood concentration predictions, as well as, a more detailed representation of the structure of the skin.

Unknown Parameters	Optimized Values
P_{sc}	0.003
P_{ve}	7.50
P_{cd}	14.99
$R_{sc/air}$	120.00
$R_{ve/air}$	102.00
$R_{cd/air}$	65.50
Sum of Squared Deviations	0.060

Table 4.15   DBM Three Layered Subcompartment Liquid Model Estimated Parameters

4.4.4   Parallel Subcompartment Liquid Model.   The unknown subcompartment permeability constants and partition coefficients of the parallel subcompa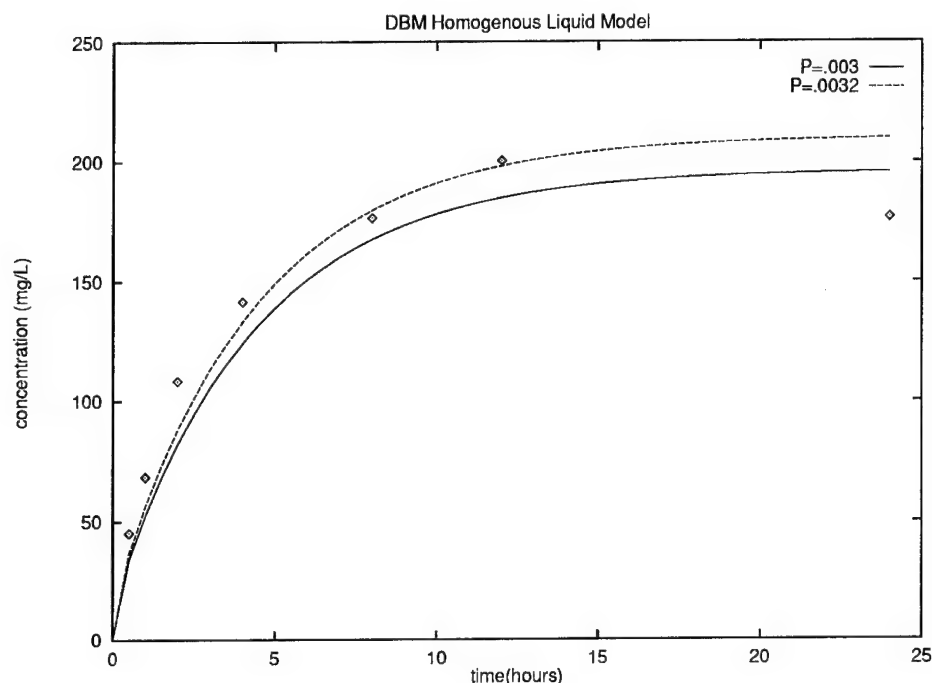rtment model were optimized and the optimized parameter values can be seen in Table 4.16. The parallel subcompartment model made better predictions than the homogeneous model and the layered subcompartment models. The parallel subcompartment model resulted in a sum of squared deviations of 0.054 which is a 45 percent improvement over the homogeneous model. Figure 4.9 shows how well the
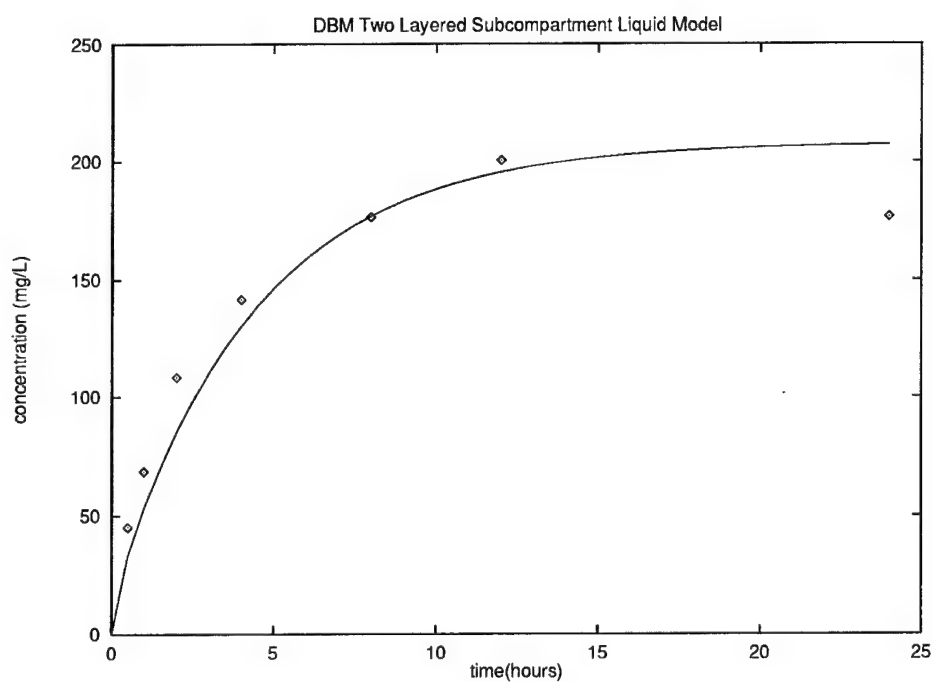
Figure 4.8 DBM Three Layered Subcompartment Liquid Model Results. This graph shows how the model's predictions compare to the experimental data.

predicted blood concentration values of the parallel subcompartment model match the experimental data.

Unknown Parameters	Optimized Values
P_{fo}	0.07
P_{cd}	0.002
$R_{fo/air}$	271.67
$R_{cd/air}$	66.58
Sum of Squared Deviations	0.054

Table 4.16   DBM Parallel Subcompartment Liquid Model Estimated Parameters
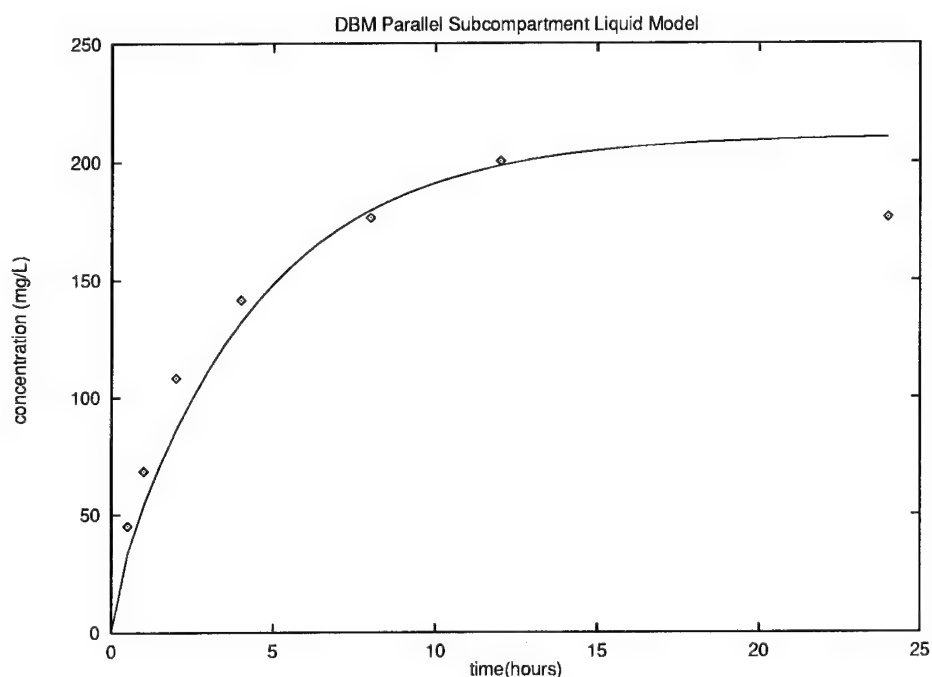
Figure 4.9   DBM Parallel Subcompartment Liquid Model Results.   This graph shows how the model's predictions compare to the experimental data.

4.4.5   Parallel-Layered Subcompartment Liquid Model.   The unknown subcompartment permeability constants and partition coefficients of the parallel-layered subcompartment model were optimized and the optimized parameter values can be

seen in Table 4.17. The parallel-layered subcompartment model made better blood concentration predictions than the homogeneous model and the layered subcompartment models, but not quite as well as the parallel subcompartment model. The parallel-layered subcompartment model resulted in a sum of squared deviations of 0.058 which is a 41 percent improvement over the homogeneous mo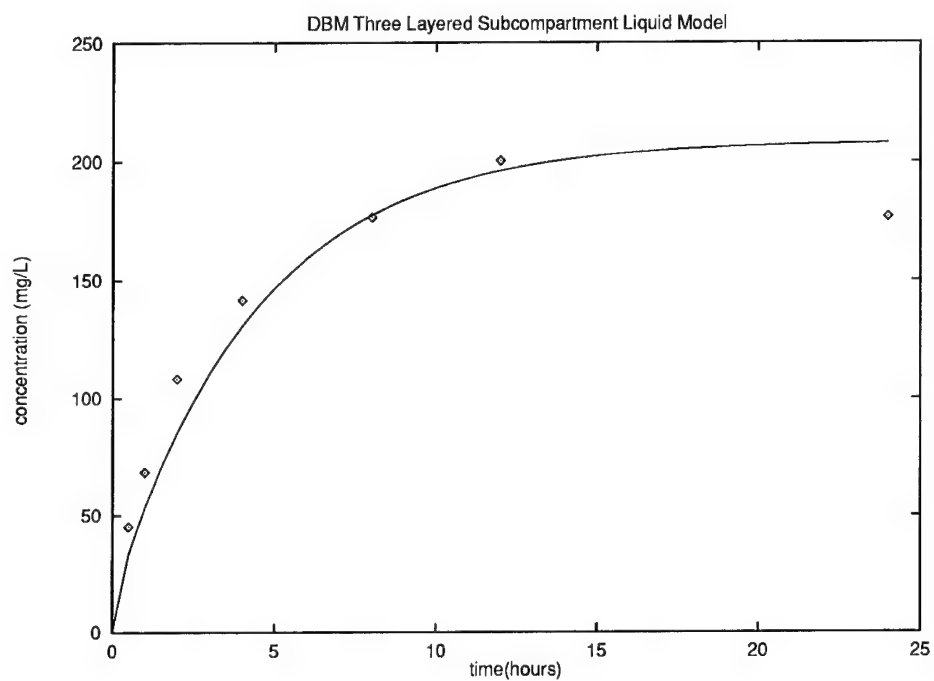del. Figure 4.10 shows how well the predicted blood concentration values of the parallel-layered subcompartment model match the experimental data.

Unknown Parameters	Optimized Values
P_{fo}	0.07
P_{sc}	0.002
P_{cd}	5.13
$R_{fo/air}$	271.67
$R_{sc/air}$	146.47
$R_{cd/air}$	64.98
Sum of Squared Deviations	0.058

Table 4.17   DBM Parallel-Layered Subcompartment Liquid Model Estimated Parameters

4.5 Sensitivity Analysis for Liquid Models

We conducted sensitivity analysis on the parameters of the skin compartments of each model to determine the impact they have on the predicted blood concentration (Tables 4.18–4.22). We looked at the percent change in predicted blood concentrations at one-half hour and at twenty four hours for each change in the parameters. In each of the models, the predicted blood concentration was the most sensitive to changes in one of the subcompartment permeability constants. The parameters of the mass-balance equations for body compartments other than the skin had relatively the same sensitivity as they did in the vapor model. Increasing the parameters by five percent had relatively the same effect as decreasing the parameter
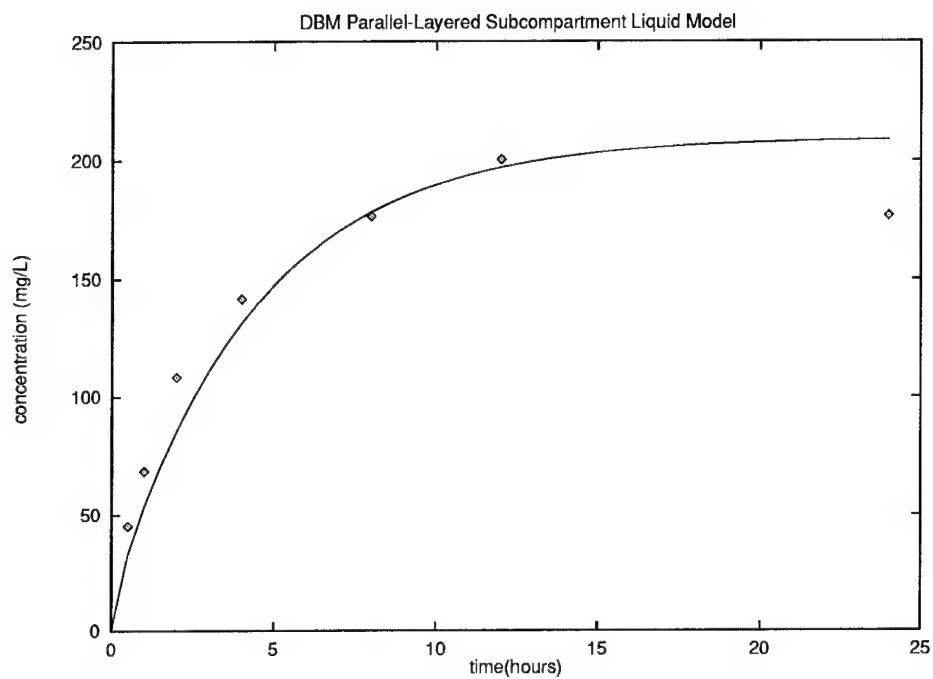
Figure 4.10   DBM Parallel-Layered Subcompartment Liquid Model Results. This graph shows how the model's predictions compare to the experimental data.
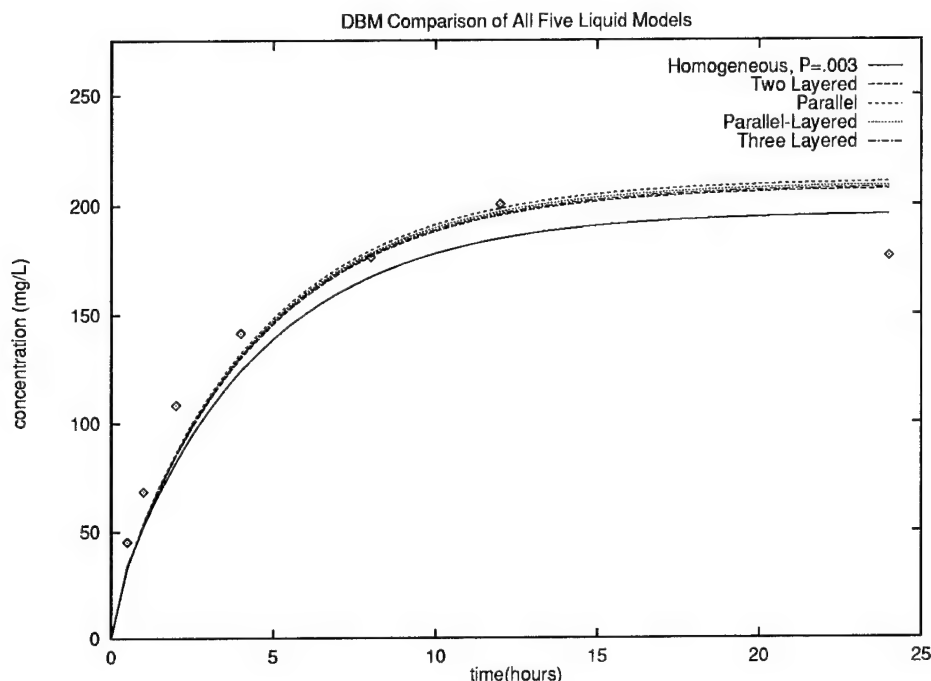
Figure 4.11   DBM Comparison of the Results of All Five Liquid Models. This graph shows how the model's predictions compare to the experimental data.

by five percent, although the direction was different. The rest of this discussion will pertain to the effect of increasing the parameters by five percent.

4.5.1   Homogeneous Liquid Model.   In the homogeneous model, the order of sensitivity was permeability (P), blood air partition coefficient $(R_{b/air})$, skin air partition coefficient $(R_{sk/air})$, and flow to the skin (Q_{sk}) (Table 4.18). Increasing the permeability, the skin air partition coefficient, and the flow to the skin increased the predicted blood concentration by nearly equivalent percentages during a one-half hour exposure and during a twenty four hour exposure. Opposite of the vapor model, changes in the blood air partition coefficient had a greater effect after twenty four hours than after one-half hour.

4.5.2   Two Layered Subcompartment Liquid Model.   In the two layered subcompartment model, changing the permeability for stratum corneum (P_{sc}) had

Parameter	.5 hours +5%	24 hours +5%
P	5.6	5.6
$R_{b/air}$	1.3	5.1
$R_{sk/air}$	-0.8	-0.8
Q_{sk}	0.8	0.8

Table 4.18 Sensitivity Analysis for the DBM Homogenous Liquid Model. These numbers represent the percent change in predicted blood concentrations after the parameters were varied.

the largest impact on the predicted blood concentration while the composite dermal permeability (P_{cd}) had practically no effect (Table 4.19). This was because P_{cd} is so large compared to P_{sc} that a five percent change in P_{cd} resulted in a very small change in the overall permeability of the skin from Equation (3.4), but a five percent change in P_{sc} resulted in about a five percent change in the overall permeability. In contrast, the predicted blood concentration was more sensitive to changes in the composite dermal partition coefficient ($R_{cd/air}$) than it was to changes in the stratum corneum partition coefficient ($R_{sc/air}$). As in the homogeneous model, the blood air partition coefficient ($R_{b/air}$) had a greater effect after twenty four hours than after one-half hour. In this model, the composite dermal partition coefficient and the blood flow to the skin (Q_{sk}) had more impact on the blood concentration after one-half hour than after twenty four hours, because the concentration difference between air and skin was diminished after twenty four hours.

4.5.3 Three Layered Subcompartment Liquid Model. In the three layered subcompartment model, like the two layered subcompartment model, changing the permeability for stratum corneum (P_{sc}) had a much larger impact on the predicted blood concentration than the permeability of the viable epidermis (P_{ve}) and the composite dermal (P_{cd}) (Table 4.20). When these parameters were estimated, the composite dermal and the viable epidermis permeabilities were significantly larger

Parameter	.5 hours +5%	24 hours +5%
P_{sc}	5.8	5.8
$R_{b/air}$	1.4	4.8
Q_{sk}	0.9	0.5
$R_{cd/air}$	-0.5	0.1
P_{cd}	0.1	0.1
$R_{sc/air}$	0.0	0.0

Table 4.19   Sensitivity Analysis for the DBM Two Layerd Subcompartment Liquid Model. These numbers represent the percent change in predicted blood concentrations after the parameters were varied.

than the stratum corneum permeability. This caused a five percent change in P_{cd} and P_{ve} to change the overall permeability of the skin by only a small percent through Equation (3.8) which resulted in a very low sensitivity for P_{cd} and P_{ve}. On the other hand, the composite dermal air partition coefficient ($R_{cd/air}$) was the only subcompartment partition coefficient to have any effect on the predicted blood concentration when changed. The effect of changing the blood flow to the skin (Q_{sk}) was greater after one-half hour than after twenty four hours. As in all of the liquid models, the blood air partition coefficient had a larger effect after one-half hour than after twenty four hours.

4.5.4   Parallel Subcompartment Liquid Model.   In the parallel subcompartment model, changing the permeability of the composite dermal subcompartment (P_{cd}) had the largest effect on the predicted blood concentrations probably because it contains the stratum corneum (Table 4.10). The blood air partition coefficient ($R_{b/air}$) had the next largest impact which is consistent with the layered subcompartment models. The permeability of the follicle subcompartment (P_{fo}) had the next largest impact which is probably because it acts as its own small skin compartment having the chemical enter from the surface and leave to the blood. The composite dermal air partition coefficient ($R_{cd/air}$) was more sensitive than the folli-

Parameter	.5 hours +5%	24 hours +5%
P_{sc}	5.8	5.8
$R_{b/air}$	1.4	4.8
Q_{sk}	0.9	0.4
$R_{cd/air}$	-0.5	0.0
P_{ve}	0.0	0.0
$R_{ve/air}$	0.0	0.0
$R_{sc/air}$	0.0	0.0
P_{cd}	0.0	0.0

Table 4.20   Sensitivity Analysis for the DBM Three Layered Subcompartment Liquid Model. These numbers represent the percent change in predicted blood concentrations after the parameters were varied.

cle air partition coefficient ($R_{fo/air}$) which was probably due to the small fractional area of the follicle subcompartment (10^{-2}). The flow to the composite dermal (Q_{cd}) subcompartment had about the same effect as the flow to the composite dermal subcompartments of the layered models, but the flow to the follicle (Q_{fo}) subcompartment had a somewhat lower sensitivity.

Parameter	.5 hours +5%	24 hours +5%
P_{cd}	4.4	4.5
$R_{b/air}$	1.4	4.8
P_{fo}	1.5	1.4
Q_{cd}	0.9	0.3
$R_{cd/air}$	-0.6	0.0
Q_{fo}	0.1	0.1
$R_{fo/air}$	-0.1	-0.1

Table 4.21   Sensitivity Analysis for the DBM Parallel Subcompartment Liquid Model. These numbers represent the percent change in predicted blood concentrations after the parameters were varied.

4-26

4.5.5 Parallel-Layered Subcompartment Liquid Model. In the parallel-layered subcompartment model, changing the permeability of the stratum corneum subcompartment (P_{sc}) had the largest effect on the predicted blood concentrations (Table 4.22). After the blood air partition coefficient $(R_{b/air})$, the permeability of the follicle subcompartment (P_{fo}) had the next largest effect on the blood concentration predictions. Since the permeability of the composite dermal subcompartment (P_{cd}) is relatively large compared to P_{sc}, changing P_{cd} by five percent actually changed the overall permeability of the non-follicle skin subcompartment by a very small percent because of Equation (3.21). The stratum corneum air $(R_{sc/air})$ and follicle air $(R_{fo/air})$ partition coefficients had relatively no impact when varied. The remaining parameters had the same order of sensitivity and relatively the same magnitudes of sensitivity as in the parallel subcompartment model.

Parameter	.5 hours +5%	24 hours +5%
P_{sc}	4.3	4.4
$R_{b/air}$	1.4	4.8
P_{fo}	1.5	1.4
Q_{cd}	0.9	0.3
$R_{cd/air}$	-0.5	0.0
Q_{fo}	0.1	0.1
$R_{sc/air}$	0.0	0.0
$R_{fo/air}$	0.0	0.0
P_{cd}	0.0	0.0

Table 4.22   Sensitivity Analysis for the DBM Parallel-Layered Subcompartment Liquid Model. These numbers represent the percent change in predicted blood concentrations after the parameters were varied.

4.6   Summary

The vapor and liquid models were used with parameters from studies involving dibromomethane (DBM). The results from all of the models were compared, by graphical plots and calculating the sum of squared deviations, to the experimental

data that was previously collected in the laboratory . The subcompartment models were an improvement over the homogeneous models. We cannot make any comparisons between the vapor and liquid models in this research because different values for the DBM parameters were used when the two original models were developed. Sensitivity analysis shows how changing the skin subcompartment parameters effect the blood concentration predictions.

V. Summary and Conclusions

5.1 Summary

The goal of this research was to develop a dermal PBPK model with multiple dermal subcompartments that improved prediction of mammalian blood concentrations of a chemical following dermal vapor or neat liquid exposure and provide the capability to predict the concentration of chemicals in distinct parts of the skin. This research resulted in the development of four new models which were adjusted to handle vapor and neat liquid exposures. A two layered subcompartment, three layered subcompartment, parallel subcompartment, and parallel-layered subcompartment model was developed. These new models were derived from previously developed homogeneous models. The predictions of all of the models were compared to the experimental data in which rats were exposed to dibromomethane vapor and neat liquid dibromomethane in doses and time durations matching those used in the models. Sensitivity analysis of the models' parameters showed which parameters are the most important to identify.

5.2 Conclusions

Each new model in turn predicted blood concentrations of dibromomethane more accurately than the original homogeneous models especially at the beginning of the exposures. The early time periods, before the chemical concentration in the blood reaches steady-state, are the most important to model because most realistic exposures will not last for extended periods of time. The new models also represent the structure of the skin in more detail, making the new models more physiologically correct. The improvement in prediction of the three subcompartment models (three layered or parallel-layered) over the two subcompartment models (two layered or parallel) was not nearly as great as the improvement of the two subcompartment models over the homogeneous models. The simplest model that works should be used, and

this argues for one of the two subcompartment models (two layered or parallel). Choice of model really depends on the chemical being modeled, the purpose of the model, and whether the additional model parameters for the three subcompartment models can readily be measured or estimated.

Sensitivity analysis provided insight into the most important parameters to measure or estimate. For these dermal exposures, changing the skin subcompartment parameters had more impact on the predicted blood concentrations than changing the parameters in the other body compartments of the model. In all four models, one of the permeability constants was the most sensitive to change, followed by the blood air partition coefficient. These parameters should be concentrated on the most when measuring or estimating parameters for these types of models.

Prediction of therapeutic or toxic events in the skin requires an understanding of the distribution of chemicals in the skin. Expanded biologically-based skin models such as these could be used as the basis for predicting efficacy of a drug which might act differently in specific parts of the skin. These models might also be used to predict deleterious dermal effects such as dermatitis or contact sensitization. Mechanistic understanding of the therapeutic or toxic events, as well as, their concentration dependence will be required, but physiologically-based pharmacokinetic models such as these would be the first step. Validation of model predictions for chemical concentration in the skin subcompartments is necessary and should be accomplished for several chemicals with different properties and at different exposure doses and durations before this model can be used mechanistically.

Permeability constants and partition coefficients for the new subcompartments were estimated or optimized in these new models. It is essential to be able to experimentally determine these parameters if the ability of a model to extrapolate to humans is to be maintained. Measuring the partition coefficients for the skin subcompartments involves technical challenges which probably can be overcome, however currently we can constrain the subcompartment partition coefficients by

the overall skin air partition coefficient using the relationship of Equation (2.8). Measurement of permeability constants for each subcompartment is probably not possible, however constraining the estimates by the overall permeability constant according to the series relationships shown in Equations (2.5) and (2.6) will not be a problem since the overall permeability can be estimated using the model.

Biologically-based models have tremendous potential to provide species, dose, and duration extrapolations of laboratory experiments. Success in these endeavors could have a big impact on pharmacology and toxicology. The strength of these models is that they can be predictive, as well as, descriptive. But, the keys to accurate prediction are a sound biological basis, and including only parameters in the model which can be measured (or estimated if absolutely necessary) in laboratory animals and in humans. These models with biologically-based subcompartments provide improved fit to the data with the potential for species extrapolation after appropriate measurements of human parameters.

5.3   Recommendations

A vapor exposure model using the same chemical parameters presented in the neat liquid homogeneous model would allow a comparison between the improvements of the subcompartment models for different types of exposure. The application of the models developed in this research to chemicals with different properties could give some insight on how chemicals with certain properties penetrate the skin.

The technique of using subcompartments to represent tissue compartments, which are identified in a model, can be used in future research to more accurately represent other tissue compartments and the complex functions that take place within them. For example, the process of metabolism and chemical binding could more accurately be represented.

Appendix A. Symbols for Equations

The following is a complete list of the symbols used in the equations in this thesis.

D = Average membrane diffusion coefficient (distance^2 time^{-1})

x = Distance

J_s = Steady-state flux of solute (moles distance^{-2} time^{-1})

δ = membrane thickness (cm)

ΔC_s = Concentration difference of solute across membrane (moles cm^{-3})

K_m = (Solute sorbed per cc of tissue)/(Solute in solution per cc of solvent)

k_p = Permeability constant (distance/time)

a = arterial

A = area (distance^2)

al = alveolar

b = blood

C = concentration (mass/volume)

c = cardiac

f = fat

i = tissue compartment i

K = Michaelis constant - metabolism (mass/volume)

k_f = first-order metabolic rate constant (time^{-1})

l = liver

P = permeability (distance/time)

p = pulmonary

A-1

Q = flow (volume/time)

R = partition coefficient (ratio of concentrations)

rp = rapidly perfused

sfc = surface

sk = skin

sp = slowly perfused

t = time

V = volume

v = venous

V_{max} = maximum reaction velocity (mass/time)

sc = stratum corneum

cd = composite dermal

ve = viable epidermis

fo = Follicle

lq = Liquid

SSD = Sum of squared deviations

n = Number of experimental data points

$TABS$ = Total amount absorbed

AM = Amount (mass)

ex = Exhaled

met = Metabolized

Bibliography

1. T. R. Auton, J. D. Ramsey, and B. H. Woollen. Modelling Dermal Pharmacokinetics Using *in vitro* Data Part I. Fluazifop-butyl in the Rat. *Human and Experimental Toxicology*, 12:199–206, 1993.

2. Gene Barnett and Vojtech Licko. Transport Across Epithelia. A Kinetic Evaluation. *International Journal of Biochemistry and Biophysics*, 464:276–286, 1977.

3. Richard L. Burden and Douglas J. Faires. *Numerical Analysis*. Prindle, Weber, and Schmidt, Boston, third edition, 1985.

4. M. Corroller, J. R. Didry, G. Siou, and J. Wepierre. Sebaceous Accumulation of Linoleic Acid following Topical Application in the Hairless Rat and Its Mathematical Treatment. *Pharmacol. Skin*, 1:111–120, 1987.

5. J. Crank. *The Mathematics of Diffusion*. Oxford Univ. Press, London, 1957.

6. Gy. A. Csanady, A. L. Mendrala, R.J. Nolan, and J. G. Filser. A physiologic pharmacokinetic model for styrene and styrene-7,8-oxide in mouse, rat, and man. *Archives of Toxicology*, 68(3):143–157, 1994.

7. Gordon L. Flynn. Mechanism of Percutaneous Absorption from Physiochemical Evidence. In Robert L. Bronaugh and Howard I. Maibach, editors, *Percutaneous Absorption. Mechanisms–Methodology–Drug Delivery*, chapter 3, pages 27–51. Marcel Dekker, Inc., New York, second edition, 1989.

8. J. M. Gearhart, D. A. Mahle, R. J. Greene, C. S. Seckel, C. D. Flemming, J. W. Fisher, and H. J. Clewell III. Variability of physiologically based pharmacokinetic (PBPK) model parameters and their effects on PBPK model predictions in a risk assessment for perchloroethylene (PCE). *Toxicology Letters*, 68:131–144, May 1993.

9. M. Gibaldi and D. Perrier. *Pharmacokinetics*. Marcel Dekker, New York, 1982.

10. Richard H. Guy and Jonathan Hadgraft. Physicochemical Interpretation of the Pharmacokinetics of Percutaneous Absorption. *Journal of Pharmacokinetics and Biopharmaceutics*, 11(2):189–203, 1983.

11. Richard H. Guy and Jonathan Hadgraft. Pharmacokinetic Interpretation of the Plasma Levels of Clonidine Following Transdermal Delivery. *Journal of Pharmaceutical Sciences*, 74(9):1016–1018, September 1985.

12. Richard H. Guy, Jonathan Hadgraft, and Howard I. Maibach. A pharmacokinetic model for percutaneous absorption. *International Journal of Pharmaceutics*, 11:119–129, 1982.

13. D. M. Hetrick, A. M. Jarabek, and C. C. Travis. Sensitivity Analysis for Physiologically Based Pharmacokinetic Models. *Journal of Pharmacokinetics and Biopharmaceutics*, 19(1):1–20, 1991.

14. Frederique Hueber, Jacques Wepierre, and Hans Schaefer. Role of Transepidermal and Transfollicular Routes in Percutaneous Absorption of Hydrocortisone and Testosterone: *In vivo* Study in the Hairless Rat. *Skin Pharmacology: the Official Journal of the Skin Pharmacology Society*, 5:99–107, 1992.

15. Brigitte Illel, Hans Schaefer, Jacques Wepierre, and Oliver Doucet. Follicles Play and Important Role in Percutaneous Absorption. *The Journal of Pharmaceutical Sciences*, 80(5):424–427, 1991.

16. Gary W. Jepson. Armstrong Laboratory, Toxicology Division. Personal Correspondence, 18 April 1995.

17. J. Kao, J. Hall, and G. Helman. *In vitro* Percutaneous Absorption in Mouse Skin: Influence of Skin Appendages. *Toxicology and Applied Pharmacology*, 94:93–103, 1988.

18. J. C. Keister and G. B. Kasting. The Use of Transient Diffusion to Investigate Transport Pathways Through Skin. *The Journal of Controlled Release*, 4:111–117, 1986.

19. Christopher R. McDaniel. Physiologically Based Pharmacokinetic Modelling of Percutaneously Absorbed Dibromomethane Utilizing Multiple Dermal Sub-Compartments. Master's thesis, Air Force Institute of Technology, September 1993.

20. James N. McDougal. Armstrong Laboratory, Toxicology Division. Personal Correspondence, 18 April 1995.

21. James N. McDougal. Physiologically Based Pharmacokinetic Modeling. In F.N. Marzulli and H. I. Maibach, editors, *Dermatotoxicology*, chapter 2, pages 37–60. Hemisphere Publishing Corporation, 1991.

22. James N. McDougal, Gary W. Jepson, Harvey J. Clewell III, and Melvin E. Andersen. Dermal Absorption of Dihalomethane Vapors. *Toxicology and Applied Pharmacology*, 79:150–158, 1985.

23. James N. McDougal, Gary W. Jepson, Harvey J. Clewell III, Michael G. MacNaughton, and Melvin E. Andersen. A Physiological Pharmacokinetic Model for Dermal Absorption of Vapors in the Rat. *Toxicology and Applied Pharmacology*, 85:286–294, 1986.

24. James N. McDougal, David Mattie, and Gary Jepson. Species Differences in Skin Penetration. Research Proposal 1, 01 October 1992 - 30 September 1995. Toxicology Division, Occupational and Environmental Health Directorate, Armstrong Laboratory, Wright-Patterson AFB, OH.

25. S. Monash and H. Blank. Location and formation of the epithelial barrier to water vapor. *Arch. Dermatol.*, 78:710–714, 1958.

26. William Montagna and Paul F. Parakkal. *The Structure and Function of the Skin.* Academic Press, New York, third edition, 1974.

27. Hirokazu Okamoto, Fumiyoshi Yamashita, Kyoko Saito, and Mitsuru Hashida. Analysis of Drug Penetration Through the Skin by the Two-Layer Skin Model. *Pharmaceutical Research*, 6(11):931–937, 1989.

28. Dennis W. Quinn. A Banach Space Solution of an Abstract Cauchy Problem Which Has Robin Boundary Data. *Quarterly of Applied Mathematics*, XLIX(1):179–200, March 1991.

29. John C. Ramsey and Melvin E. Andersen. A Physiologically Based Description of the Inhalation Pharmacokinetics of Styrene in Rats and Humans. *Toxicology and Applied Pharmacology*, 73:159–175, 1984.

30. R. F. Rushmer, K. J. K. Buettner, J. M. Short, and G. F. Odland. The Skin. *Science*, 154:343–348, 1966.

31. Kiyoshi Sato, Kenji Sugibayashi, Yasunori Morimoto, Harumi Omiya, and Naoyoshi Enomoto. Prediction of the In-vitro Human Skin Permeability of Nicorandil form Animal Data. *J. Pharm. Pharmacol.*, 41(6):379–383, June 1989.

32. H. Schaefer, A. Zesch, and G. Stuttgen. *Skin Permeability*. Springer-Verlag, Berlin, 1982.

33. Hans Schaefer and Chris Hensby. Skin Permeability and Models of Percutaneous Absorption. In Corrado L. Galli, Christopher N. Hensby, and Marina Marinovich, editors, *Skin pharmacology and toxicology: recent advances*, pages 77–83, New York, 1990. NATO Scientific Affairs Division, Plenum Press.

34. R. J. Scheuplein. On the application of rate theory to complex multibarrier flow co-ordinates: membrane permeability. *J. Theoret. Biol.*, 18:72–89, 1968.

35. Robert J. Scheuplein. Mechanism of Percutaneous Absorption II. Transient Diffusion and the Relative Importance of Various Routes of Skin Penetration. *The Journal of Investigative Dermatology*, 48(1):79–88, 1967.

36. Robert J. Scheuplein and Irvin H. Blank. Permeability of the Skin. *Physiological Reviews*, 51(4):702–744, October 1971.

37. Robert C. Scott, Maureen A. Corrigan, Fiona Smith, and Helen Mason. The Influence of Skin Structure on Permeability: An Intersite and Interspecies Comparison with Hydrophilic Penetrants. *The Journal of Investigative Dermatology*, pages 921–925, June 1991.

38. Jane E. Shaw, Mary Prevo, Robert Gale, and Su II Yum. Percutaneous Absorption. In Lowell A. Goldsmith, editor, *Physiology, Biochemistry, and Molecular Biology of the Skin*, volume II, chapter 55, pages 1447–1479. Oxford University Press, New York, second edition, 1991.

39. L. J. Shyr, P. J. Sabourin, M. A. Medinsky, L. S. Birnbaum, and R. F. Henderson. Physiologically Based Modeling of 2-Butoxyethanol Disposition in Rats Following Different Routes of Exposure. *Environmental Research*, 63:202–218, 1993.

40. O. Siddiqui, M. S. Roberts, and A. E. Polack. Percutaneous Absorption of Steroids: Relative Contributions of Epidermal Penetration and Dermal Clearance. *Journal of Pharmacokinetics and Biopharmaceutics*, 17(4):405–424, 1989.

41. P. Singh and M. S. Roberts. Skin Permeability and Local Tissue Concentrations of Nonsteroidal Anti-Inflammatory Drugs after Topical Application. *The Journal of Pharmacology and Experimental Therapeutics*, 268(1):144–151, January 1994.

42. C. C. Travis. Interspecies Extrapolation in Risk Analysis. *Ann. Ist. Super. Sanita*, 27(4):581–593, 1991.

43. R. T. Tregear. Relative Penetrability of Hair Follicles and Epidermis. *The Journal of Physiology*, 156:307–313, 1961.

44. Jan E. Wahlberg. Transepidermal or Transfollicular Absorption? *Acta Dermato-venereologica*, 48:336–344, 1968.

45. Sylvia M. Wallace and Gene Barnett. Pharmacokinetic Analysis of Percutaneous Absorption: Evidence of Parallel Penetration Pathways for Methotrexate. *The Journal of Pharmacokinetics and Biopharmaceutics*, 6(4):315–325, 1978.

46. Ronald C. Wester and Howard I. Maibach. Regional Variation in Percutaneous Absorption. In Robert L. Bronaugh and Howard I. Maibach, editors, *Percutaneous Absorption. Mechanisms–Methodology–Drug Delivery*, chapter 7, pages 111–119. Marcel Dekker, Inc., New York, 1989.

47. Fumiyoshi Yamashita, Tamaki Yoshioka, Yasuo Koyama, Hirokazu Okamoto, Hitoshi Sezaki, and Mitsuru Hashida. Analysis of Skin Penetration Enhancement Based on a Two-Layer Skin Diffusion Model with Polar and Nonpolar Routes in the Stratum Corneum: Dose-Dependent Effect of 1-Geranylazacycloheptan-2-one on Drugs with Different Lipophilicities. *Biol. Pharm. Bull.*, 16(7):690–697, July 1993.

Vita

Lt Bookout was born in Houston, Texas on 15 July 1971. He grew up in Owasso, Oklahoma where he graduated from high school in 1989. He attended the United States Air Force Academy in Colorado Springs, Colorado and graduated with a Bachelor of Science in Mathematics in 1993.

Lt Bookout's first assignment was to attend the Air Force Institute of Technology (AFIT) in residence at Wright-Patterson Air Force Base, Dayton, Ohio to complete a Master of Science in Computer Systems.

Lt Bookout is married to the former Ms Carrie Ojala who is from Owasso, Oklahoma.

Permanent address: 12110 Coulson Circle
Houston, Texas 77015

REPORT DOCUMENTATION PAGE

Form Approved
OMB No. 0704-0188

1. AGENCY USE ONLY (Leave blank)	2. REPORT DATE	3. REPORT TYPE AND DATES COVERED
	June 1995	Master's Thesis

4. TITLE AND SUBTITLE

Physiologically-Based Pharmacokinetic Modeling of Skin Absorption Using Dermal Subcompartments

5. FUNDING NUMBERS

6. AUTHOR(S)

Richard Lynn Bookout Jr., First Lieutenant, USAF

7. PERFORMING ORGANIZATION NAME(S) AND ADDRESS(ES)

AFIT/ENC
Wright-Patterson AFB, OH 45433

8. PERFORMING ORGANIZATION REPORT NUMBER

AFIT/GCS/ENC/95J-01

9. SPONSORING / MONITORING AGENCY NAME(S) AND ADDRESS(ES)

AAMRL/OET
Wright-Patterson AFB, OH 45433

10. SPONSORING / MONITORING AGENCY REPORT NUMBER

11. SUPPLEMENTARY NOTES

12a. DISTRIBUTION / AVAILABILITY STATEMENT

Distribution Unlimited

12b. DISTRIBUTION CODE

13. ABSTRACT (Maximum 200 words)

Dermal penetration of chemicals and drugs is important to both toxicologists and pharmacologists. Drug developers try to enhance and environmental professionals try to limit penetration of chemicals through the skin. Both can use predictive biologically-based mathematical models to assist in understanding the processes involved. When these models are based on physiological and biochemical parameters which can be measured in the laboratory, they can be extremely useful. Appropriately validated models based on first principles can be predictive of human exposures when the processes involved are adequately understood. In this thesis we develop four new physiologically-based pharmacokinetic (PBPK) models to predict blood concentrations of dibromomethane (DBM) in rats after neat liquid and vapor exposure. These four new models expand previously developed homogeneous models by adding skin subcompartments. These new models improve the prediction of the blood concentrations. Sensitivity analysis shows that one of the permeability constants followed by the blood air partition coefficient have the most impact on blood concentration predictions.

14. SUBJECT TERMS

Physiologically-Based Pharmacokinetic Modeling, Dermal Subcompartments, Dermal Absorption

15. NUMBER OF PAGES

88

16. PRICE CODE

17. SECURITY CLASSIFICATION OF REPORT	18. SECURITY CLASSIFICATION OF THIS PAGE	19. SECURITY CLASSIFICATION OF ABSTRACT	20. LIMITATION OF ABSTRACT
unclassified	unclassified	unclassified	UL

NSN 7540-01-280-5500

Standard Form 298 (Rev. 2-89)
Prescribed by ANSI Std. Z39-18
298-102